

PEOPLE'S DEMOCRATIC REPUBLIC OF ALGERIA
MINISTRY OF HIGHER EDUCATION AND SCIENTIFIC RESEARCH
UNIVERSITY OF M'SILA – MOHAMED BOUDIAF

FACULTY OF SCIENCES
DEPARTEMENT OF PHYSICS

N° :...../2024



FIELD: Material Sciences

PROGRAM: Physics

OPTION : THEORITICAL PHYSICS

Thesis submitted for the attainment of
Master's Degree

By: ABDAT Mohamed hocine

Title :

High energy physics modeling

Dark Matter search

Board of Examiners :

BOUSSAHEL Mounir	Université de M'sila	President
REDOUANE SALAH Essma	Université de M'sila	Supervisor
DEBABI Mourad	Université de M'sila	Examiner

2024/2023

REPUBLIQUE ALGERIENNE DEMOCRATIQUE ET POPULAIRE
MINISTRE DE L'ENSEIGNEMENT SUPERIEUR ET DE LA RECHERCHE
SCIENTIFIQUE
UNIVERSITE MOHAMED BOUDIAF -M'SILA

FACULTE DES SCIENCES
DEPARTEMENT PHYSIQUE

N°...../2024



DOMAINE : Sciences de la matière
FILIERE : Physique
OPTION : PHYSIQUE THEORIQUE

**Mémoire présenté pour L'obtention
Du Diplôme de Master Académique**

Par: Mohamed Abdat Hocine

Intitulé:

**Modélisation de la Physique des Hautes Énergies
Recherche de La Matière Sombre**

Soutenu le 13/06/2024 devant le jury composé de:

Boussahel Mounir	Université de M'sila	Président
Redouane Salah Essma	Université de M'sila	Rapporteur
Debabi Mourad	Université de M'sila	Examineur

Année universitaire : 2024/2023

Dedication

I wholeheartedly dedicate this work to:

My beloved parents, whose support and sacrifices have been the backbone of my success.

My teacher, Redouane Salah Essma, and all other teachers whose guidance has been invaluable.

The dear friends I made through this journey, who are no less than brothers to me.

All those who share the same passion for physics and work to unravel the secrets of our universe.

Acknowledgements

I offer my deepest gratitude to:

My teacher and supervisor, Redouane Salah Essma, for her guidance and encouragement. Much respect and appreciation to you.

All the teachers who aided me in finishing this research.

My friends and family who supported me and helped me during my journey.

The administration of our department who provided the right environment for scientific research and acquiring knowledge.

Contents

1 Introduction	7
1.1 Historical Background	8
1.2 Evidence of Dark Matter :	9
1.3 Cosmological standard model and Dark Matter :	11
1.4 Dark matter candidates :	12
1.5 Essential Aspects of Dark Matter Particle Detection :	13
1.5.1 Relic density	13
1.5.2 Direct detection :	14
1.5.3 Indirect detection :	15
1.5.4 Dark Matter Production in Colliders	16
2 Standard Model and Dark Matter	17
2.1 The Standard Model of Particle Physics :	18
2.2 The Standard Model and its limitations	19
2.3 Particle dark matter candidates :	20
2.4 Simplified Dark Matter models :	21
2.4.1 Simplified Dark matter model with spin-0 mediator Y_0	21
2.4.2 Simplified Dark matter model with a spin-1 mediator Y_1^μ	22
2.4.3 Simplified dark matter model with a spin-2 mediator $Y_2^{\mu\nu}$:	23
3 Dark Matter Experimental searches :	26
3.1 Cosmological experiments :	27
3.2 Direct Detection experiments :	28
3.3 Indirect Detection experiments :	30
3.4 Production in colliders :	30
4 Simulation of Simplified Dark Matter models spin-0/spin-1/spin-2	32
4.1 Introduction:	33
4.2 Installation:	33
4.3 MadDM :	34
4.4 Relic density and Direct Detection of Simplified Dark Matter Model with spin-0 mediator Y_0 :	35
4.4.1 Fermionic dark matter particles candidate X_d :	35
4.4.2 Real Scalar Dark Matter particles candidate X_r :	39
4.4.3 Complex scalar dark matter particles candidate X_c :	41
4.5 Relic density of Simplified Dark matter model with spin-1 mediator Y_1^μ	45
4.5.1 Fermionic dark matter particles candidate X_d :	45
4.5.2 Complex Scalar dark matter particles candidate X_c :	45

4.6	Relic density of Simplified Dark matter model spin-2 mediator $Y_2^{\mu\nu}$	46
4.6.1	Fermionic dark matter particles candidate X_d	46
4.6.2	Real Scalar Dark matter particles candidate X_r	46
4.6.3	Vector Dark matter particles candidate X_v	47
4.6.4	Discussion	48
5	Simulation of Dark Matter production in Colliders	50
5.1	Introduction	51
5.2	Simplified Dark matter model spin-0 mediator Y_0	51
5.3	Simplified Dark matter model spin-1 mediator Y_1^μ	52
5.4	Simplified Dark matter model spin-2 mediator $Y_2^{\mu\nu}$	53
5.5	Neutrinos missing energy	54
5.6	Discussion	55
5.6.1	Spin-0 Mediator Y_0	55
5.6.2	Spin-1 Mediator Y_1^μ	55
5.6.3	Spin-2 Mediator $Y_2^{\mu\nu}$	55
5.6.4	Comparison with Neutrinos in the SM	56
5.7	Conclusion	56

List of Figures

1.1	Anomaly between expected and observed speeds	5	8
1.2	Hubble telescope at a striking example of gravitational lensing	10	9
1.3	Setup of a Gravitational Lens	10	10
1.4	Large-scale Structure of the Universe from Illustris Simulator	12	10
1.5	Percentage of Dark Energy and Dark Matter and ordinary matter	14	11
1.6	NASA/WMAP Timeline of the universe	15	12
1.7	Dark matter candidates mass ranges	27	13
1.8	interaction of DM and SM	37	16
2.1	The Standard Model elementary particles		19
2.2	Elementary particles in simplified Dark matter models as SM extensions		25
3.1	The anisotropies of the Cosmic Microwave Background (CMB)	60	28
3.2	The Lrge Hadron Collider	82	31
4.1	Installation steps for MadGraph.		33
4.2	Packages Installation process in MadGraph.		34
4.3	Ahnillation proces of X_d into a pair of top-antitop quarks		36
4.4	The variations of relic density with respect to the mass M_{X_d}		36
4.5	Scattering proces up + $X_d = \text{up} + X_d$		37
4.6	Comparison of Direct Detection Cross-Sections		38
4.7	Ahnillation proces of X_r into W^+ and W^-		39
4.8	variations of DM scalar type's relic density with respect to mass M_{X_r}		39
4.9	Scattering process between down-quark and X_r		40
4.10	Comparison of Direct Detection Cross-Sections for M_{X_r}		41
4.11	Ahnillation process of X_c particles into pair of two higgs bosons		42
4.12	The variations of relic density with respect to M_{X_c}		43
4.13	Scattering process between down-quark and X_c		43
4.14	Comparison of Direct Detection Cross-Sections for M_{X_c}		44
4.15	The variations of Relic density with respect to MX_d		45
4.16	The variations of Relic density with respect to MX_c		45
4.17	The variations of Relic density with respect to MX_d		46
4.18	Variations of Relic density with respect to MX_R		47
4.19	Variations of Relic density with respect to MX_V		47
5.1	The proces $bb \rightarrow \gamma \rightarrow xd + xd + jet$		51
5.2	MET of DM in spin-0		52
5.3	The proces $q\bar{q} \rightarrow Y \rightarrow X_d + X_d + jet$		52
5.4	MET of DM in spin-1		53

5.5	proces $q\bar{q} \rightarrow \gamma^0 \rightarrow x + \bar{x} + jet$	53
5.6	MET of DM in spin-2	54
5.7	Missing Energy of SM's neutrinos	54

Chapter 1

Introduction

1.1 Historical Background

In the 1930s the Swiss astronomer Fritz Zwicky^[1], observed galaxy clusters and calculate the mass and found it to be on the order of $10^{15}M_{\odot}$, but from the spectrum analysis, he found it to be on the order of $10^{13}M_{\odot}$. where M_{\odot} is the mass of the sun, He noticed a discrepancy between the visible mass and the mass needed to hold clusters together gravitationally. He proposed the presence of unseen matter he called it in German "*Dunkle Materie*" in English Dark Matter which mean i doesn't interact with light, However, his ideas faced skepticism initially. Meanwhile, theoretical work by Jan Oort^[2] and others considered the possibility of existence of non-luminous matter in the Milky way,

In the 1970s, Vera Rubin^[3], along with collaborator Kent Ford, conducted observations of spiral galaxies. They focused on measuring the rotation curves of these galaxies, which describe how the orbital velocity of stars and gas changes with their distance from the center of the galaxy, According to classical Newtonian physics or Einstein's general relativity^[4], one would expect the rotation curves of galaxies to follow a certain pattern: the orbital velocities should decrease with increasing distance from the galactic center. However, Rubin's observations revealed something unexpected — the velocities did not drop off as predicted. Instead, the rotation curves remained roughly constant or even increased with distance from the center.

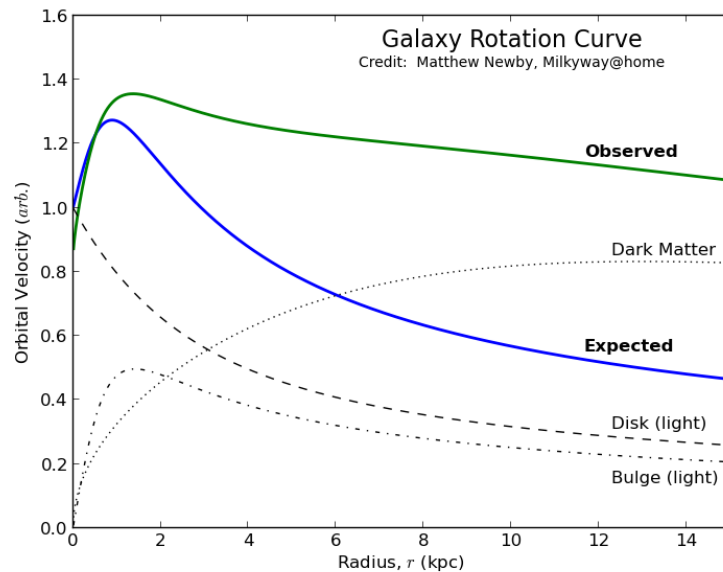


Figure 1.1: Anomaly between expected and observed speeds^[5]

This discrepancy between the observed rotation curves and the predictions based on visible matter (stars and gas) led to the proposal that there must be a significant amount of unseen matter, or "dark matter," influencing the gravitational dynamics of galaxies. The presence of this invisible mass was crucial to explaining the observed rotation curves.

1.2 Evidence of Dark Matter :

In the context of the Λ CDM¹ model^[6], dark matter plays a crucial role in explaining several key phenomena observed in the universe like :

1. **Galaxy Rotation Curves:** Dark matter helps explain the observed rotation curves of galaxies. In spiral galaxies, the rotational velocities of stars and gas do not decrease as expected with increasing distance from the galactic center^[3]. Instead, they remain relatively constant or even increase. Dark matter's gravitational influence provides the additional mass necessary to produce these observed rotation curves.
2. **Cosmic Microwave Background (CMB):** Dark matter contributes to the fluctuations observed in the cosmic microwave background radiation^[7], which is the remnant radiation from the early universe. These fluctuations provide valuable insights into the initial conditions of the universe and the distribution of matter and energy.
3. **Gravitational Lensing:** Dark matter causes gravitational lensing^[8], where the gravitational field of massive objects bends the paths of light rays passing nearby, This effect allows astronomers to indirectly detect^[9] and map the distribution of dark matter in the universe by observing its gravitational influence on light from distant objects.

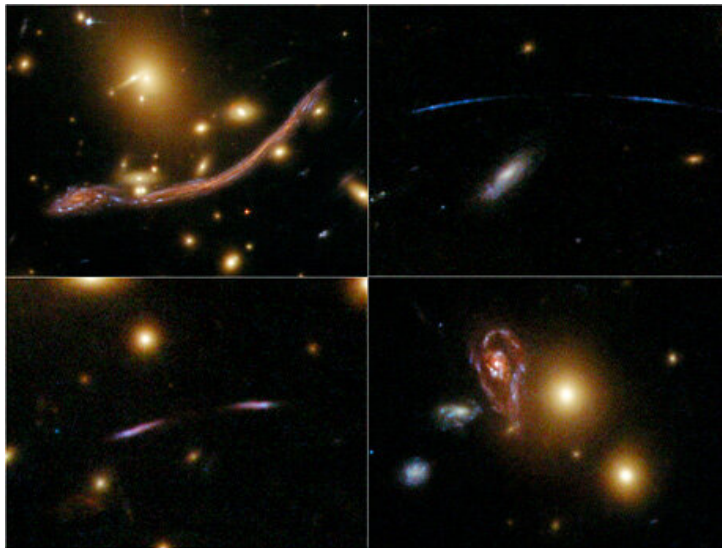


Figure 1.2: Hubble telescope at a striking example of gravitational lensing^[10]

¹This is sometimes called the Cosmological Standard model, that combines the cosmological constant λ with cold dark matter (CDM). It explains the evolution of the universe from the Big Bang to its current state

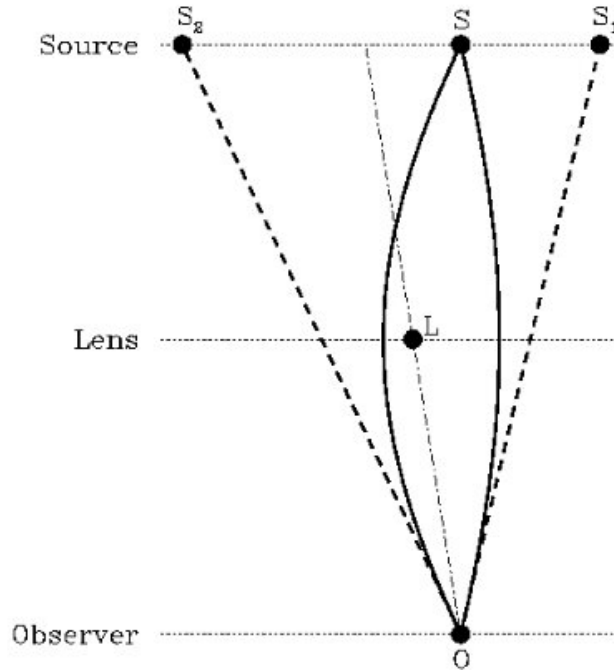


Figure 1.3: Setup of a Gravitational Lens [10]

4. **Large-Scale Structure:** Dark matter is thought to be the dominant form of matter in the universe, comprising approximately 27% of its total energy density (compared to about 5% for ordinary matter). Its gravitational pull influences the large-scale distribution of galaxies and galaxy clusters [11], shaping the cosmic web of filaments and voids observed in large-scale structure surveys.

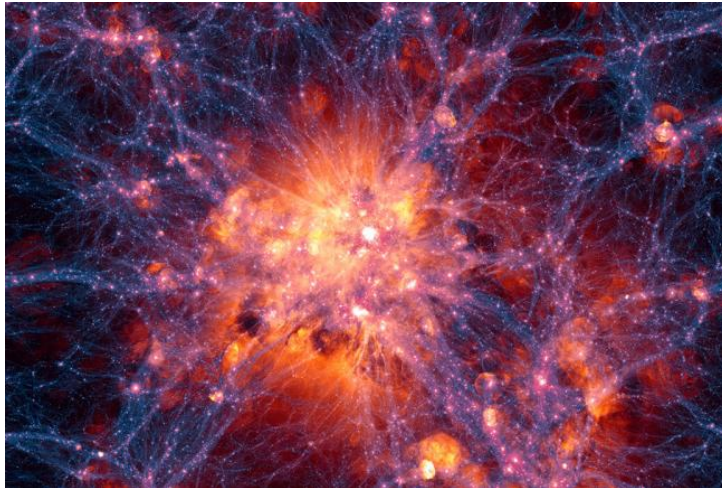


Figure 1.4: Large-scale Structure of the Universe from Illustris Simulator [12]

5. **Cosmic Acceleration:** In the Λ CDM model, dark energy (represented by the cosmological constant Λ) is responsible for the observed accelerated expansion of the universe. However, dark matter's gravitational effects provide the necessary "clumping" to allow the formation of galaxies and other cosmic structures despite this expansion.

1.3 Cosmological standard model and Dark Matter :

The cosmological observations indicates that before 13.7 billion years ago the universe began with the big bang from a very hot and dense point called the singularity, Initially, the universe existed in a state of quark-gluon plasma, where matter and radiation were in thermal equilibrium. As it cooled, quarks combined to form protons. However, nuclei could not form immediately because the photon energy was comparable to the binding energy between nucleons (protons and neutrons). Only when the universe cooled further nuclei began to form [13], The current amount of dark matter in the Universe is known as the relic density of dark matter. after 380000 years from the big bang the temperature was $3000 \text{ K} \approx 1 \text{ eV}$ the atoms formed, This temperature allows protons and electrons to bind without constantly being ionised by photons, this makes photons free, these are the first photons emitted in the Universe can be detected as a microwave signal coming from all directions, and that's what we call Cosmic Microwave Background (CMB) [7] because of the redshift they became in the range of microwave and a temperature of 2.73 K . The Universe comprises radiation, matter, and vacuum. The total energy density Ω is the sum of all components:

$$\Omega = \Omega_{\text{rad}} + \Omega_{\text{m}} + \Omega_{\Lambda} \quad (1.1)$$

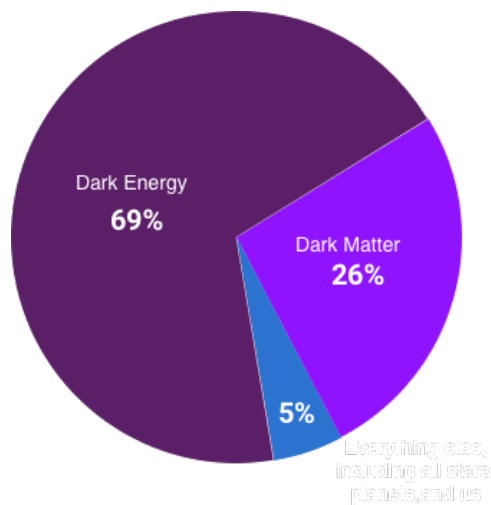


Figure 1.5: Percentage of Dark Energy and Dark Matter and ordinary matter [14]

Where Ω_{rad} , Ω_{m} , and Ω_{Λ} are the energy densities of radiation, matter, and vacuum (dark energy), respectively. Current measurements indicate that $\Omega_{\Lambda} \approx 0.68$ and $\Omega_{\text{m}} \approx 0.32$, with the matter content divided into baryonic density $\Omega_{\text{baryon}} \approx 0.05$ and dark matter density $\Omega_{\text{c}} \approx 0.27$. This implies that 83% of the total matter is dark matter, while ordinary matter constitutes only 17%, The densities are given in terms of h^2 , a quantity related to the Hubble parameter H_0 , which measures the expansion rate of the Universe. The Hubble parameter is defined as $H_0 = \frac{v}{d}$. it is relates to h as $h = H_0/100 \text{ km}/(\text{s Mpc})$. Current estimates give $h = 0.67$. Given the dark matter density $\Omega_{\text{DM}} = 0.27$, And $\Omega_{\text{DM}}h^2 = 0.12$.

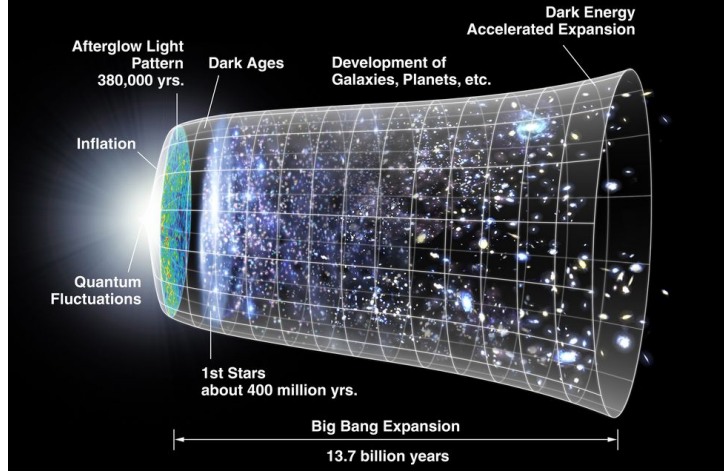


Figure 1.6: NASA/WMAP Timeline of the universe [15]

1.4 Dark matter candidates :

There are some other theories that predict DM candidates, Modified Newtonian dynamics **MOND** that try to explain the velocity of rotating galaxies, MOND actually is not a dark matter candidate but the biggest DM's competitor, it tries to find a solution to the problem of hidden mass without invisible matter, MOND is an alternative theory of gravity proposed by Milgrom in the 1980s [16]. It suggests a modification to Newtonian dynamics at low accelerations, typically below $a_0 \approx 10^{-10} \text{ m/s}^2$. The theory introduces a function, often denoted as $\mu(a/a_0)$, to modify the gravitational force law, it can expressed as:

$$F = m\mu\left(\frac{a}{a_0}\right)a \quad (1.2)$$

Where F is the gravitational force, m is the mass of an object, a is the acceleration, and a_0 is a fundamental acceleration scale, MOND provides an alternative explanation for the dynamics of galaxies and galaxy clusters without the need for dark matter [17].

However, MOND faces challenges in explaining certain cosmological observations [18], such as the large-scale structure of the universe and the cosmic microwave background (CMB). Also, MOND has difficulty explaining the observed tidal features, while dark matter simulations naturally produce such structures. We can mention that the observed orbits of satellite galaxies around larger galaxies do not align well with MOND predictions [19].

Primordial Blackholes : Primordial black holes [20] are theorized to be potential candidates for dark matter, suggesting that they may constitute a significant fraction of the elusive dark matter in the universe.

Massive Compact Halo Objects (MACHOs): are faint or non-luminous astronomical objects in the galaxy's halo. They have low luminosity, making them difficult to detect with current telescopes [21]. MACHOs can be baryonic [22], like primordial black holes [20] formed early in the Universe, or brown dwarfs, which are hydrogen-rich but too

low in mass to start hydrogen fusion. Although these objects may account for some dark matter, their non-observation and constraints suggest they do not constitute the primary component of dark matter, MACHOs maybe detected through gravitational microlensing [23] [24], where the MACHO's gravity bends the light from a star behind it, causing the star to appear brighter.

Elementary particles Dark Matter : Particle dark matter refers to the hypothesis that dark matter consists of elementary particles [25] [26], the Standard Model of particle physics is incomplete as we will see in details the [Section 2.2], undiscovered particles may exist beyond it. These new particles, predicted by various theories [25], could possess the properties required to be dark matter candidates. A DM particle must be sufficiently long-lived, potentially as old as the Universe, and multiple types of new particles from different models could collectively constitute dark matter.

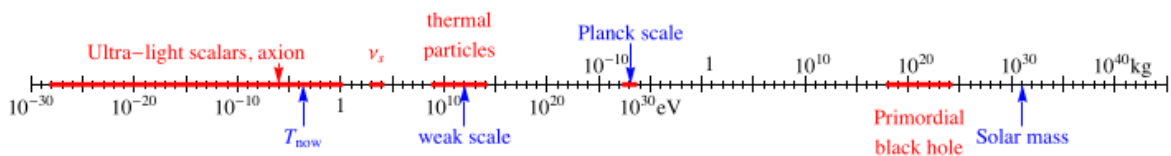


Figure 1.7: Dark matter candidates mass ranges [27]

1.5 Essential Aspects of Dark Matter Particle Detection :

1.5.1 Relic density

In cosmology, the term “relic density” [28] refers to the present quantity of a given elementary particle that remains from the Big Bang. It’s a measure of how much of that particle exists in the universe today compared to when the universe was very young. In the context of dark matter, relic density is often modeled for weakly interacting massive particles (WIMPs), which are a leading candidate for dark matter. The relic density of dark matter is important because it helps scientists understand the amount of dark matter that should exist in the universe. If dark matter particles were in thermal equilibrium in the early universe, their relic density can be calculated using the Boltzmann equation. The relic density of dark matter is often calculated in the context of specific models [29]. For example, in the Inert Doublet Model (IDM) [30] [31], the relic density of dark matter is calculated at one-loop, The density evolution equation [32] [33] determines the relic density for a dark matter candidate X .

$$\frac{dn_X}{dt} + 3Hn_X = -2 \langle \sigma_{\text{eff}} v \rangle \left(n_X^2 - (n_X^{EQ})^2 \right), \quad (1.3)$$

where $\sigma_{\text{eff}} v$ is the effective thermally averaged annihilation cross section times velocity, h is the Hubble expansion constant, and n_X is the number density of dark matter particles, and n_X^{EQ} is the equilibrium number density of the dark matter particles

$$\langle \sigma_{\text{eff}} v \rangle \equiv \sum_{i,j=1}^N \langle \sigma (\chi_i \chi_j \rightarrow SM) v \rangle \frac{n_{x_i}^{EQ} n_{x_j}^{EQ}}{\left(n_X^{EQ} \right)^2} \quad (1.4)$$

$$\langle \sigma_{\chi\bar{\chi} \leftrightarrow X\bar{X}} |v\rangle = \frac{2Tm_x^2}{(2\pi)^4 n_{eq}^2 (1 + \delta_{\chi\bar{\chi}})} \int_0^1 d\beta \frac{\beta}{(1 - \beta^2)^2} \times \sqrt{\frac{\lambda(s, m_\chi^2, m_{\bar{\chi}}^2)}{s}} K_1\left(\frac{\sqrt{s}}{T}\right) W_{ij}(s) \quad (1.5)$$

where k runs over all the particles in the process, while n_χ^{EQ} is the thermal equilibrium density of the dark matter species with mass m_χ and g_χ internal degrees of freedom at temperature T :

$$n_\chi^{EQ} \approx g_\chi \left(\frac{m_\chi T}{2\pi}\right)^{3/2} e^{-m_\chi/T} \quad (1.6)$$

K_1 is the modified Bessel function of the second kind, $\beta \equiv \sqrt{1 - 4m_\chi^2/s}$ is the relativistic velocity of the initial state particles, while the numerically convenient W_{ij} proxy is defined as:

$$W_{ij}(s) = \frac{\sqrt{\lambda(s, m_X^2, m_{\bar{X}}^2)}}{(1 + \delta_{X\bar{X}}) 8\pi s} \int \sum_{spins} |\mathcal{M}|^2 \left(\frac{d\Omega_{CM}}{4\pi}\right) \quad (1.7)$$

where $\lambda(a, b, c)$ is the usual two-body kinematic function:

$$\lambda(a, b, c) \equiv a^2 + b^2 + c^2 - 2(ab + bc + ac)$$

Notice that the definition of effective thermally averaged cross section reduces to $\langle \sigma(\chi\chi \rightarrow SM) |v\rangle$ in case of only one dark matter particle and no-coannihilating partners.

and in with the hubble constant :

$$\Omega_{DM} h^2 \approx \frac{1.07 \times 10^9 \text{ GeV}^{-1} x_f}{g_*^{1/2} M_{Pl} \langle \sigma v \rangle} \quad (1.8)$$

- M_{Pl} : The Planck mass, approximately 1.22×10^{19} GeV.
- x_f : The freeze-out parameter, defined as $x_f = \frac{m_{DM}}{T_f}$, where m_{DM} is the mass of the dark matter particle and T_f is the freeze-out temperature.
- g_* : The effective number of relativistic degrees of freedom at the time of freeze-out.
- $\langle \sigma v \rangle$: The thermally averaged annihilation cross section of the dark matter particles.

The relic density is an important parameter in cosmology and the study of dark matter. It provides a link between the microphysics of particle interactions and the large-scale structure of the universe, by comparing the calculated relic density of a dark matter model with the observed dark matter density in the universe

1.5.2 Direct detection :

Dark matter (DM) direct detection [\[34\]](#) refers to a set of experimental techniques and theoretical methodologies aimed at observing interactions between dark matter particles and ordinary matter. Unlike indirect detection, which looks for byproducts of dark matter annihilations or decays, direct detection experiments aim to detect dark matter particles directly as they pass through or interact with a detector material, Direct detection experiments are informed by various dark matter models, including Weakly Interacting Massive Particles (WIMPs), axions, and other hypothetical particles

spin-independent (SI) scattering cross section:

$$\sigma_{SI} = \frac{4}{\pi} \mu_A^2 \cdot [Z \cdot f_p + (A - Z) \cdot f_n]^2,$$

where $\mu_A = \frac{m_\chi m_A}{m_\chi + m_A}$ is the DM-nucleus reduced mass and f_p and f_n are proton/neutron spin independent form factors respectively [11, 13, 27]. We use Z to denote the number of protons in a nucleus and A to denote the number of protons and neutrons. Similarly.

spin-dependent (SD) scattering cross section:

$$\sigma_{SD} = \frac{16}{\pi} \mu_A^2 \cdot \frac{J_A + 1}{J_A} (f'_p + f'_n)^2,$$

where f'_p and f'_n are the proton/neutron spin-dependent form factors respectively, and J_A is the spin of the nucleus. Particle physics enters the calculation of $\sigma_{SD/SI}$ via the form factors f_N and f'_N where $N = p, n$.

The differential event rate $\frac{dR}{dE_R}$ for dark matter-nucleus scattering is given by:

$$\frac{dR}{dE_R} = \frac{\rho_\chi}{m_\chi} \int_{v_{\min}}^{v_{\max}} f(v) \frac{d\sigma}{dE_R} v dv$$

where: ρ_χ is the local dark matter density and m_χ is the mass of the dark matter particle and $f(v)$ is the velocity distribution of dark matter particles, and $\frac{d\sigma}{dE_R}$ is the differential cross-section for dark matter-nucleus scattering, and E_R is the recoil energy, and v_{\min} and v_{\max} are the minimum and maximum velocities of the dark matter particles that can produce a recoil of energy E_R .

1.5.3 Indirect detection :

Searching for dark matter indirectly involves looking for the byproducts of interactions between dark matter particles [35] rather than directly finding dark matter particles themselves. Finding dark matter's annihilation or decay products [36], such as neutrinos, gamma rays, or cosmic rays, is the main goal. Indirect detection can be approached in several ways:

- **Annihilation of dark matter:** If the particles that make up dark matter are their own antiparticles, then they can annihilate one another to produce particles that are detectable, such as neutrinos, gamma rays, or cosmic rays. Experiments look for an overabundance of these particles in areas where the density of dark matter is high.
- **Dark matter decay :** If dark matter is unstable, it will eventually break down into particles that can be observed.
- **Cosmic ray electrons and positrons :** Measurements of the cosmic ray electron and positron spectrum by experiments like Fermi-LAT have shown intriguing features that could potentially come from dark matter annihilation or decay

The mass, lifetime, and dark matter annihilation cross section are all constrained by indirect searches. Differentiating dark matter signals definitively from astrophysical backgrounds such as pulsars can be difficult, though. Any potential dark matter signals discovered through indirect detection will need to be confirmed by consistency across various experiments and additional measurements.

1.5.4 Dark Matter Production in Colliders

Dark matter production in colliders, such as the Large Hadron Collider (LHC), is a crucial area of research in particle physics. In these experiments, high-energy proton-proton collisions are utilized to recreate conditions similar to those just after the Big Bang. The aim is to produce dark matter particles, which would manifest as missing energy in the detector since they interact very weakly with ordinary matter. Researchers look for events with significant missing transverse energy, along with other particles that could indicate the presence of dark matter. Despite extensive searches, no direct evidence of dark matter production has been observed so far, but these experiments continue to refine our understanding of potential dark matter properties and guide future searches.

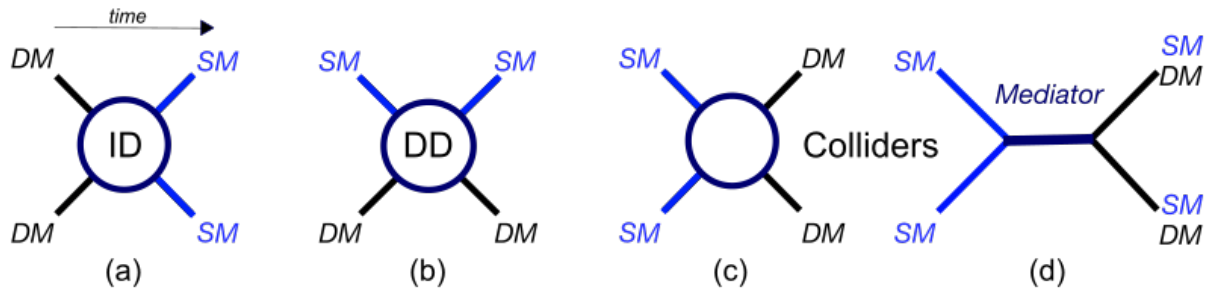


Figure 1.8: interaction of DM and SM 37

interaction of DM particles and SM particles with
a) Indirect Detection , b) Direct Detection , c) DM production in colliders

Chapter 2

Standard Model and Dark Matter

2.1 The Standard Model of Particle Physics :

The standard model of particle physics [38] [39] is a quantum field theory [40] that describes the fundamental particles, quarks, leptons, and gauge bosons and their interactions via the three fundamental quantized forces: electromagnetic, weak, and strong forces. The SM successfully explains most experimental results and predicts a wide range of phenomena. The most comprehensive theory now available to scientists to explain the fundamental components of the universe is the Standard Model of Particle Physics [41]. It describes the way that the visible matter is composed of particles called fermions, which include electrons, and quarks, which make up protons and neutrons. It also describes how the quarks and leptons are affected by force carrying particles, which are a type of bosons. Three of the four fundamental forces that control the universe -electromagnetism, the strong force, and the weak force- are explained by the Standard Model. Photons carry electromagnetic force, which is the result of the a combination of magnetic and electric fields. Atomic nuclei are bound together by the strong force, which is carried by gluons, to create stability. The W and Z bosons are carrying the weak force. The last one is responsible of nuclear reactions that have powered the Sun and other stars for billions of decades, The SM can explain all observed phenomena in particle colliders at a wide range of energies, Gravity is the fourth fundamental force which is described by general theory of relativity at the large scale, that the Standard Model is unable to sufficiently explain, so from this and from another problems we are going to mention we can surly know that the SM is the best current theory to explain nature but it is not the final theory to describe it

The symmetry group of the standard model should be : $SU(3)_c \otimes SU(2)_I \otimes U(1)_Y$ where:

- Y represents the hypercharge,
- I is the weak isospin
- C represents the color charge.

The relation between electric charge (Q), weak isospin (I_3), and hypercharge (Y) is given by Gell-Mann–Nishijima formula: $Q = I_3 + \frac{Y}{2}$, where I_3 is the third component of isospin.

The Standard Model Lagrangian [42], given by $SU(3)_c \otimes SU(2)_I \otimes U(1)_Y$, is expressed as:

$$\mathcal{L}_{SM} = \mathcal{L}_{Gauge} + \mathcal{L}_{fermions} + \mathcal{L}_{Higgs} + \mathcal{L}_{Yukawa}$$

So the \mathcal{L}_{SM} becomes like this:

$$\begin{aligned} \mathcal{L}_{SM} = & -\frac{1}{4} F_{\mu\nu}^a F_a^{\mu\nu} \\ & + i\bar{\psi}\not{D}\psi + \text{h.c.} \\ & + \bar{\psi}_i y_{ij} \psi_j \phi + \text{h.c.} \\ & + |D_\mu \phi|^2 - V(\phi) \end{aligned} \tag{2.1}$$

In this expression, $F_{\mu\nu}^a$ represents the field strength tensor for the gauge fields ψ represents the fermion fields, ϕ is the Higgs field, and $V(\phi)$ is the Higgs potential.

D_μ The covariant derivative for a fermion field ψ

y_{ij} is the Yukawa coupling constants

The Yukawa terms refer to interactions between fermions and the Higgs field, which are crucial for understanding the masses of fundamental particles in the Standard Model of particle physics.

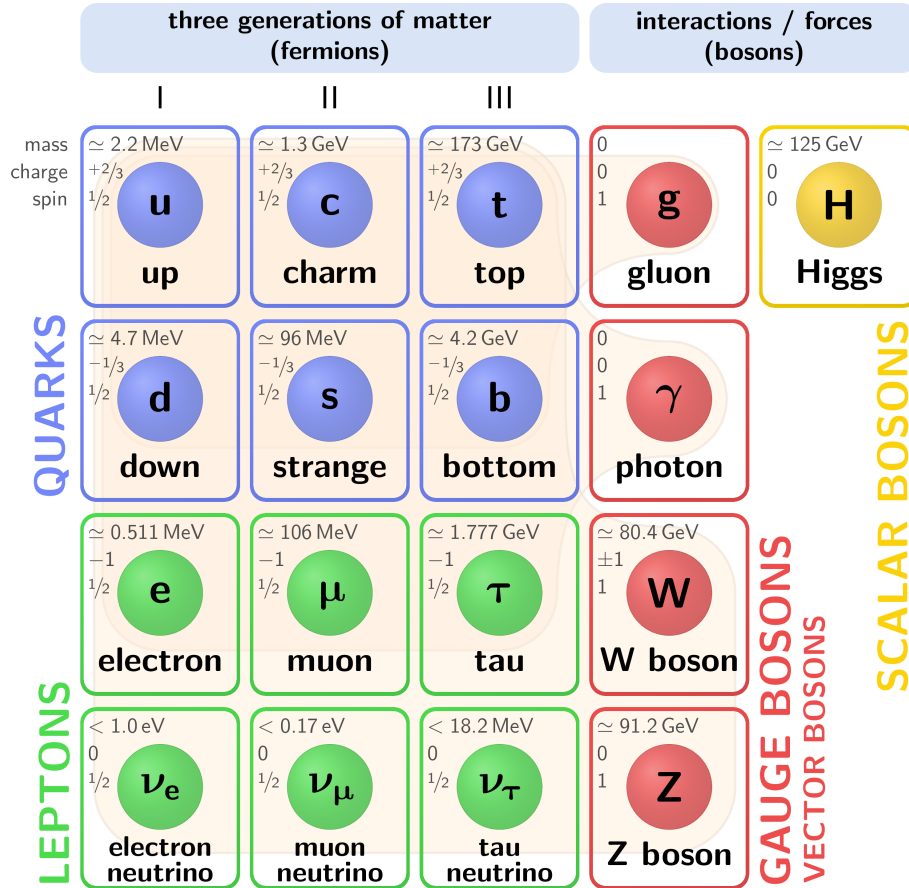


Figure 2.1: The Standard Model elementary particles

2.2 The Standard Model and its limitations

Although the SM can explain the fundamental interactions between particles and fields and many other successful predictions like Higgs boson, self-interactions of gauge bosons, and provides precise relationships between their couplings, we know that the SM is not the everything theory but an effective theory because that leaves questions unanswered [43] about some phenomena like :

- **Gravity** : The standard model can't give any description of this fundamental force [44]. As we mentioned before, this force was described successfully at large scale by the general theory of relativity as a geometrical force—bodies that are attracted to each other because of the curvature of spacetime—and not a gauge force like the other three forces. The SM is built on quantum field theory. This mathematical framework failed to find a quantization for the gravitational field and faces many ultraviolet catastrophes and the infinities, so the graviton rests as a hypothetical particle until today.

- **Matter/Antimatter asymmetry** : The matter-antimatter asymmetry problem arises from the fact that the observable universe is dominated by matter [45], while antimatter is relatively rare [46]. According to SM and QFT, matter and antimatter should have been created in equal amounts during the early universe's high-energy conditions. However, the universe we observe today is composed of matter. Understanding why this imbalance exists and how it arose shortly after the Big Bang remains an unsolved problem in SM physics.
- **Neutrino Masses** : Even after the spontaneous symmetry breaking, the neutrinos maintain their masslessness as the Standard Model does not contain right-handed neutrino fields, but from the experimental high energy physics we found that the neutrinos are not massless which was approved by the detection of neutrino oscillations [47]. This phenomena describes how neutrinos are switching their flavor between ν_e , ν_μ , and ν_τ . The Pontecorvo-Maki-Nakagawa-Sakata (PMNS) matrix, a unitary matrix that connects neutrinos' mass basis and flavor basis—in which they have a specific mass and flavor, respectively—is used to characterize it, Therefore, in order to include non-zero mass terms for the neutrinos in the Standard Model, an extension is necessary.
- **Dark Energy** : From the observations of Cosmic Microwave Background Polarization and Hubble's Law redshift we realize that our universe in cosmic expansion, depends to the cosmological calculation it represents 68% of the universe—dark energy [48] is a property of the empty spacetime itself, and it can violate the conservation law of energy, this is one of the mysterious in the SM model physics
- **Dark matter** : the Standard Model does not include any particle that fits the characteristics of dark matter [49]. Dark matter is postulated to be a form of matter that neither emits nor absorbs light or any other electromagnetic radiation, It interacts primarily through gravity, and while the SM does include particles that interact via the weak nuclear force (like neutrinos), their properties do not match those of dark matter.

2.3 Particle dark matter candidates :

as we mentioned in the introduction there are so many different candidates which try to explain this phenomena but in the particles candidates there are famous models like : **Weakly Interacting Massive Particles (WIMPs)**: WIMPs are hypothetical particles that interact weakly with ordinary matter and have masses ranging from a few times to hundreds of times that of a proton [50]. They are one of the most studied dark matter candidates and arise naturally in various extensions of the Standard Model, such as supersymmetry.

Axions: Axions [51] are hypothetical particles proposed to solve the strong CP problem [52] in quantum chromodynamics. They are also considered dark matter candidates due to their properties, such as their low mass and weak interactions with other particles.

Sterile Neutrinos: In extensions of the Standard Model involving neutrino physics, sterile neutrinos [53] are additional neutrino species that do not participate in weak interactions. Depending on their properties, sterile neutrinos could potentially account for dark matter.

Dark Photons: Dark photons [54], also known as hidden photons or paraphotons, are hypothetical gauge bosons that mediate a hidden sector force analogous to electromagnetism. If these dark photons interact weakly with ordinary matter, they could serve as dark matter candidates.

Gravitinos: Gravitinos are hypothetical supersymmetric partners of the graviton, the mediator of gravitational interactions. In certain supersymmetric models [55], gravitinos are stable and could contribute to the dark matter density.

2.4 Simplified Dark Matter models :

Simplified Dark Matter Models (SimpDM) [56] are theoretical frameworks employed within particle physics to explore and characterize potential dark matter candidates beyond the Standard Model. The primary objective of SimpDM is to simplify the complexity of dark matter models while retaining their essential features, facilitating both theoretical analysis and experimental investigation.

At its core, SimpDM typically introduces new particles or fields into the Standard Model that could serve as plausible dark matter candidates. These candidates are characterized by specific properties crucial for dark matter, such as stability over cosmological timescales, gravitational interactions with ordinary matter, and compatibility with observational constraints.

The philosophy of Simplified dark matter models [57] is to extend the Standard Model by introducing new particles and mediators in the dark sector. These models add specific interaction terms to capture the key features of dark matter interactions while keeping the framework manageable. They are designed to match experimental constraints from various sources, such as relic density measurements, direct detection experiments, and collider searches, allowing researchers to study the properties and behavior of dark matter in a controlled and simplified way.

2.4.1 Simplified Dark matter model with spin-0 mediator Y_0

We consider different types of interactions between the SM, the dark sector and the mediator [58] Y_0 [58]. The renormalizable interactions of the mediator with the DM are described by the Lagrangian [58] $\mathcal{L}_X^{Y_0}$:

$$\mathcal{L}_X^{Y_0} = \frac{1}{2} m_{X_r} g_{X_r}^s X_r X_r Y_0 + m_{X_c} g_{X_c}^s \bar{X}_c X_c Y_0 + \bar{X}_d (g_{X_d}^s + i g_{X_d}^p \gamma^5) X_d Y_0 \quad (2.2)$$

in this Lagrangian there are three different type of Dark matter particles :

- X_d is Dirac Dark matter (spinor) field
- X_c is Complex scalar Dark matter field
- X_r is Real scalar Dark Matter field

where Y_0 is the mediator of interactions between dark matter particles and the Standard Model or within the dark sector itself. In the other side the Lagrangian \mathcal{L}_{0SM} which describe interactions between Y_0 and SM particles can be written as :

$$\mathcal{L}_{SM}^{Y_0} = \sum_{i,j} \left[\bar{d}_i \frac{y_{ij}^d}{\sqrt{2}} \left(g_{d_{ij}}^S + i g_{d_{ij}}^P \gamma^5 \right) d_j + \bar{u}_i \frac{y_{ij}^u}{\sqrt{2}} \left(g_{u_{ij}}^S + i g_{u_{ij}}^P \gamma^5 \right) u_j \right] Y_0 \quad (2.3)$$

where y_i are Yukawa coupling constants

There are two coupling constants, g_{ij}^S and g_{ij}^P , because they represent two different types of interactions between the particles.

- g_{ij}^S is the scalar coupling constant, which describes interactions that are independent of the direction or polarization of the particles.
- g_{ij}^P is the pseudoscalar coupling constant, which describes interactions that depend on the direction or polarization and involve the γ_5 matrix.

Having these two types of couplings allows the model to accurately describe the various possible interactions and properties of the particles. The Lagrangian for the interaction between a gauge field and a scalar/pseudoscalar dark matter particle is given by:

$$\mathcal{L}_{\text{gauge}}^{Y_0} := \frac{1}{\Lambda} F_a^{\mu\nu} (g_S F_{\mu\nu}^a + g_P F_{\mu\nu}^a) Y_0, \quad (2.4)$$

where: - Λ is the suppression scale. - $\mathcal{F}_{\mu\nu,a}$ is the field strength tensor of the gauge field G . - $\tilde{F}_{\mu\nu,a}$ is the dual field strength tensor of G .

the simplified dark matter model scalar mediator Y_0 as extension to the standard model

:

$$\mathcal{L}_{\text{DM}}^{Y_0} = \mathcal{L}_{\text{SM}}^{Y_0} + \mathcal{L}_{\text{X}}^{Y_0} + \mathcal{L}_{\text{gauge}}^{Y_0} \quad (2.5)$$

This is a "leptophobic" model so there is no a term for interaction between between leptons and Dark sector via the Y_0 it couples just with quarks

2.4.2 Simplified Dark matter model with a spin-1 mediator Y_1^μ

the same thing with the previous model we will consider different types of interactions between the SM [58], the dark sector and the mediator Y_1 but in this case DM particles can couples to leptones and there is many diffrent between the mediator of the interaction the Lagrangian $\mathcal{L}_{\text{X}}^{Y_1}$ of coupling between DM and the mediator Y_1^μ can be written as :

$$\begin{aligned} \mathcal{L}_{\text{X}}^{Y_1} = & m_{X_c}^2 X_C^* X_C + m_{X_d} \bar{X}_d X_d \\ & + \frac{i}{2} g_{X_c}^V [X_C^* (\partial_\mu X_C) - (\partial_\mu X_C^*) X_C] Y_1^\mu + \bar{X}_d (g_{X_d}^V + i g_{X_d}^A \gamma^5) X_d Y_1^\mu \end{aligned} \quad (2.6)$$

Vector Coupling ($g_{X_d}^V$): This coupling represents the interaction between the vector part of the current and the spin-1 mediator Y_1^μ . It is associated with the term $\bar{X}_d \gamma^\mu X_d$, which is a vector current. Physically, this type of interaction affects the spatial components of the fermions field X_d , influencing how it moves and interacts spatially.

Axial-Vector Coupling ($g_{X_d}^A$): This coupling represents the interaction between the axial-vector part of the current and the spin-1 mediator Y_1^μ . It is associated with the term $\bar{X}_d \gamma^\mu \gamma^5 X_d$, which is an axial-vector current. Physically, this type of interaction affects the spin components of the fermion field X_d , influencing how the spin of X_d interacts with the mediator.

the lagrangian $\mathcal{L}_{\text{SM}}^{Y_1}$ describes the interactions between SM quarks and Y_0 mediator :

$$\mathcal{L}_{\text{SM}}^{Y_1} = \sum_{i,j} \left[\bar{d}_i \gamma_\mu (g_{d_{ij}}^V + g_{d_{ij}}^A \gamma^5) d_j + \bar{u}_i \gamma_\mu (g_{u_{ij}}^V + g_{u_{ij}}^A \gamma^5) u_j \right] Y_1^\mu \quad (2.7)$$

and the Lagrangian \mathcal{L}_{1SMlep} of coupling with leptons is :

$$\begin{aligned}
\mathcal{L}_{SMlep}^{Y_2} = & \bar{e}\gamma^\mu(g_{l11}^V + g_{l11}^A\gamma^5)eY_1^\mu \\
& + \bar{\mu}\gamma^\mu(g_{l22}^V + g_{l22}^A\gamma^5)\mu Y_1^\mu \\
& + \bar{\tau}\gamma^\mu(g_{l33}^V + g_{l33}^A\gamma^5)\tau Y_1^\mu \\
& + \nu_{11}\bar{\nu}_e\gamma^\mu(P_L)\nu_e Y_1^\mu \\
& + \nu_{22}\bar{\nu}_\mu\gamma^\mu(P_L)\nu_\mu Y_1^\mu \\
& + \nu_{33}\bar{\nu}_\tau\gamma^\mu(P_L)\nu_\tau Y_1^\mu
\end{aligned} \tag{2.8}$$

P_L in this Lagrangian represent the projector operator $P_L \equiv \frac{1}{2}(1 - \gamma^5)$ as we know there is only Left-handed neutrino

The Lagrangian for the interaction between a gauge field and a scalar/pseudoscalar dark matter particle is given by:

$$\mathcal{L}_{\text{gauge}}^{Y_1} := \frac{1}{\Lambda} F_a^{\mu\nu} \left(g^V F_{\mu\nu}^a + g^A \tilde{F}_{\mu\nu}^a \right) Y_1^\mu, \tag{2.9}$$

So the finale Lagrangian of this Model as extension becomes :

$$\mathcal{L}_{DM}^{Y_1} = \mathcal{L}_{SM}^{Y_1} + \mathcal{L}_X^{Y_1} + \mathcal{L}_{\text{gauge}}^{Y_1} + \mathcal{L}_{SMlep}^{Y_1} \tag{2.10}$$

2.4.3 Simplified dark matter model with a spin-2 mediator $Y_2^{\mu\nu}$

We consider a simplified DM models where a Dark matter candidates (X) couples to the SM particles via spin-2 mediator [\[59\]](#) :

The interaction terms between $Y_2^{\mu\nu}$ and dark matter fields X can be written as:

$$\mathcal{L}_X^{Y_2} = -\frac{1}{\Lambda} g_X^T T_{\mu\nu}^X Y_2^{\mu\nu} \tag{2.11}$$

Where Λ is the scale parameter of the theory

And g_X^T is the coupling constant between DM X and the tensor boson $Y_2^{\mu\nu}$

And $T_{\mu\nu}^X$ is the energy-momentum tensor of a DM field.

In this model we can consider three types of DM particles a real scalar (X_R), a Dirac fermion (X_D), and a vector (X_V) which is new type unlike the previous two models .

The interaction with SM particles is obtained by :

$$\mathcal{L}_{SM}^{Y_2} = -\frac{1}{\Lambda} \sum_i g_i^T T_{\mu\nu}^i Y_2^{\mu\nu} \tag{2.12}$$

Where the index i denotes each Standard model field, i.e. the Higgs doublet (H), quarks (q), leptons (ℓ), and $SU(3)_C$, $SU(2)_L$ and $U(1)_Y$ gauge bosons ($gluons$, W^+ , W^- , Z^0 , and the photon A) , $g_i^T = \{g_H^T, g_q^T, g_\ell^T, g_g^T, g_W^T, g_A^T\}$

The energy-momentum tensors of dark matter fields $T_{\mu\nu}^X$ in details will be :

$$T_{\mu\nu}^{X_R} = -\frac{1}{2}g_{\mu\nu} (\partial_\rho X_R \partial^\rho X_R - m_X^2 X_R^2) + \partial_\mu X_R \partial_\nu X_R$$

$$\begin{aligned} T_{\mu\nu}^{X_D} &= -g_{\mu\nu} (\bar{X}_D i \gamma_\rho \partial^\rho X_D - m_X \bar{X}_D X_D) + \frac{1}{2} g_{\mu\nu} \partial_\rho (\bar{X}_D i \gamma^\rho X_D) \\ &\quad + \frac{1}{2} \bar{X}_D i (\gamma_\mu \partial_\nu + \gamma_\nu \partial_\mu) X_D \\ &\quad - \frac{1}{4} \partial_\mu (\bar{X}_D i \gamma_\nu X_D) - \frac{1}{4} \partial_\nu (\bar{X}_D i \gamma_\mu X_D), \end{aligned}$$

$$T_{\mu\nu}^{X_V} = -g_{\mu\nu} \left(-\frac{1}{4} F_{\rho\sigma} F^{\rho\sigma} + \frac{m_X^2}{2} X_{V\rho} X_V^\rho \right) + F_{\mu\rho} F_\nu^\rho + m_X^2 X_{V\mu} X_{V\nu}$$

where $F_{\mu\nu}$ is the field strength tensor

Complying with the simplified-model idea, it is instructive to consider universal couplings between the spin-2 mediator and the SM particles:

Real Scalars: X_r

Spin-0 dark matter type lagrangian of coupling with $Y_2^{\mu\nu}$ will be :

$$\mathcal{L}_X^{Y_2} = -\frac{1}{\Lambda} (g_{X_r}^T T_{\mu\nu}^{X_r} Y_2^{\mu\nu})$$

Fermions: X_d

Spin $\frac{1}{2}$ dark matter type lagrangian of coupling with $Y_2^{\mu\nu}$ will be :

$$\mathcal{L}_{X_d}^{Y_2} = -\frac{1}{\Lambda} (g_{X_d}^T T_{\mu\nu}^{X_d} Y_2^{\mu\nu})$$

Vectors: X_v

Spin-1 dark matter type lagrangian of coupling with $Y_2^{\mu\nu}$ will be :

$$\mathcal{L}_{X_v}^{Y_2} = -\frac{1}{\Lambda} (g_{X_v}^T T_{\mu\nu}^{X_v} Y_2^{\mu\nu})$$

The new particles after the extensions of simpDM are illustrated in the following table :

Elementary of SM of particle physics with the extension of simplified DM models

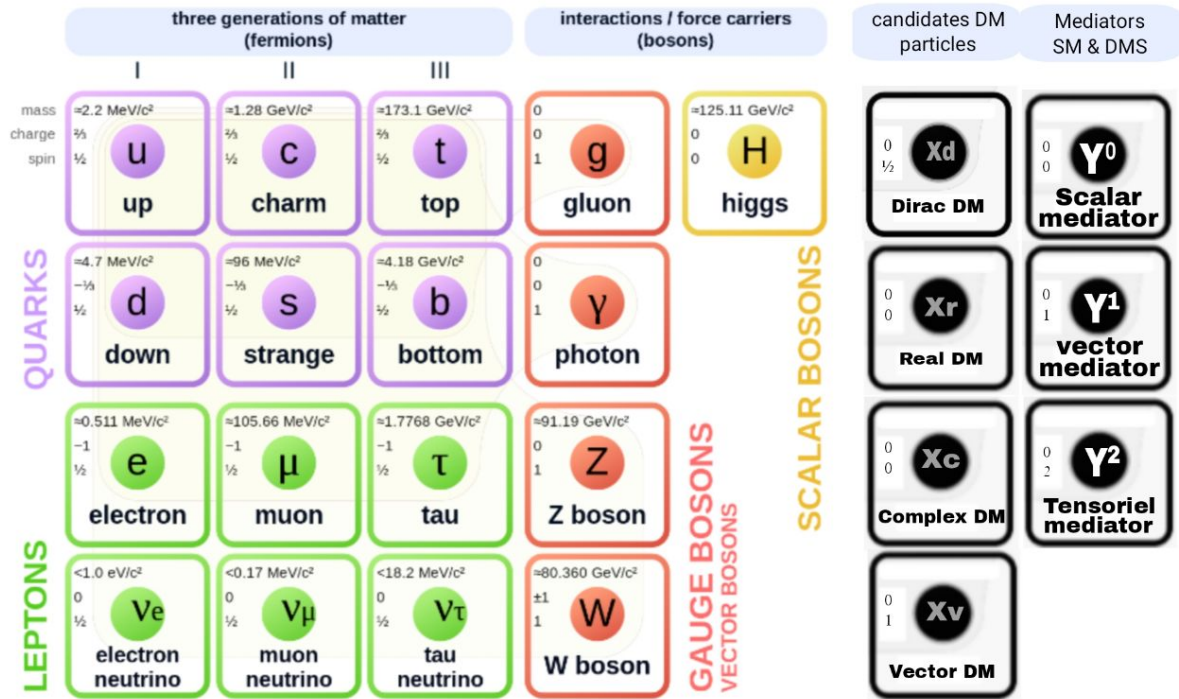


Figure 2.2: Elementary particles in simplified Dark matter models as SM extensions

Interactions between DM particle candidates and SM should be [1.8](#) as we explained in the first chapter :

Chapter 3

Dark Matter Experimental searches :

3.1 Cosmological experiments :

Galaxy clusters :

In coma cluster as an example the total mass from virial theorem (Zwicky Smith) for a self-gravitating system in equilibrium, kinetic energy T and potential energy V are related by the virial theorem : $2T + V = 0$

So the kinetic energy becomes : $T = \frac{1}{2} \sum_i m_i v_i^2$ wich means square velocity average value :

$$\langle v^2 \rangle = \frac{\sum_i m_i v_i^2}{\sum_i m_i} = \frac{2T}{M} \quad (3.1)$$

and potential energy : $V = -\frac{1}{2} \sum_i \sum_{j \neq i} \frac{G m_i m_j}{r_{ij}}$

We define gravitational radius : $R_G = 2 \left(\sum_i m_i \right)^2 \left(\sum_i \sum_{i \neq j} \frac{m_i m_j}{r_{ij}} \right)^{-1}$

So we can rewrite the potential energy $V = -\frac{GM^2}{R_G}$ then, from $2T + V = 0$, the total mass

$$: M = \sum_i m_i = \frac{R_G \langle v^2 \rangle}{G}$$

The virial theorem is important in detecting dark matter involves precise measurements of velocities, masses, and distances within clusters, revealing gravitational anomalies that cannot be explained solely by visible matter. This approach underscores the significance of gravitational dynamics in unveiling the presence and nature of dark matter in the universe.

Cosmic Microwave Background radiation :

A great resource for researching the large-scale structure of the universe is the CMB radiation. The CMB radiation's temperature variations reveal details about the early universe's density fluctuations, which are the earliest manifestations of the universe's large-scale structure.

Dark matter and CMB radiation are closely related, and understanding one requires knowledge of the other, The distribution of DM may be deduced from its effects on visible matter and the CMB radiation, which are necessary for the formation and evolution of galaxies and galaxy clusters.

On large angular scales, Temperature fluctuations : $\frac{\Delta T}{T} \sim 10^{-5}$

Fluctuations in gravitational potential (poisson equation) is given by :

$$\nabla^2(\delta\Phi) = 4\pi G \delta\epsilon \quad (3.2)$$

Redshift or blueshift for EM-waves : $\frac{\delta T}{T} = \frac{1}{3} \delta\Phi$

Sub-horizon Density perturbations in dark matter grows with the radiation-matter equality ($t \sim 0.05 \text{ Myr}$). Baryons are tightly coupled to photons until decoupling ($\sim 0.4 \text{ Myr}$) and perturbations in baryons can only grow after decoupling. Therefore in a universe without non-baryonic DM initial perturbations have to be larger ($\Delta T/T \sim 10^{-4}$)

for observed structures to form. For perturbations to grow sufficiently from initial measured amplitude, requires non-baryonic DM.

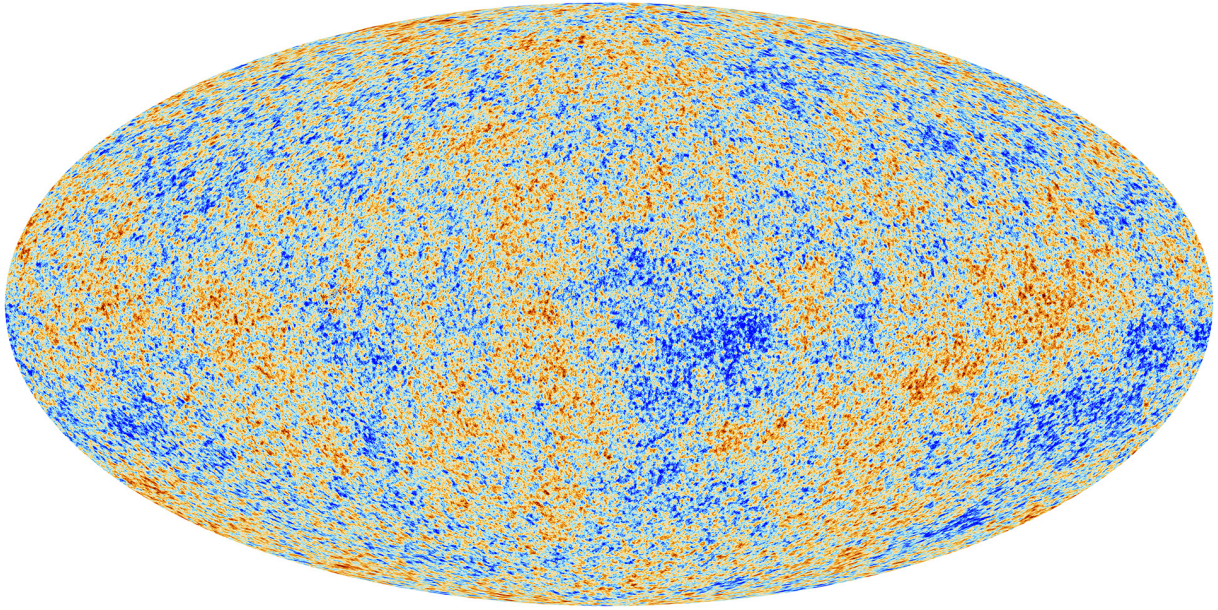


Figure 3.1: The anisotropies of the Cosmic Microwave Background (CMB) [60]

3.2 Direct Detection experiments :

XENON Experiment :

XENON experiment [61] is a direct detection dark matter experiment that uses liquid xenon as a target medium to detect the small charge and light signals produced by collisions between xenon nuclei and dark matter particles in a liquid-gas time projection chamber.

The first phase, XENON10 [62], operated at the Gran Sasso Underground Laboratory until 2007 and provided the most accurate limits on WIMP dark matter at the time. XENON100 [63], the second phase, surpassed XENON10 [62] in sensitivity and operated until early 2016.

XENON1T [64] [65], the third phase and the first tonne-scale LXe TPC for dark matter detection, ran from 2016 to 2018. It set new best limits on several physics searches and detected an unexpected excess of low-energy events.

In 2021, XENONnT [66], the latest and more advanced member of the XENON family, began operation after a swift upgrade from XENON1T. With a larger target mass and an anticipated tenfold reduction in background noise, XENONnT aims to further advance the search for dark matter in the coming years.

ORGAN: WISP Direct Detection

The Oscillating Resonant Group AxioN Experiment [67] [68], or ORGAN for short, is a type of detector known as a “haloscope,” which tries to detect dark matter axions as they pass through the laboratory [69].

Rather than relying on energy imparted when an axion collides with a standard model particle, haloscopes like ORGAN rely on what is called the axion-photon coupling [70]. Essentially, if we engineer the correct conditions inside the detector, and axions are passing through, we can force a small number of the axions to convert into photons, which are particles of light.

So, we can take the invisible dark matter and convert it into a tiny flash of light which we can then detect.

Fortunately, while we cannot see or touch dark matter directly, we can detect light. So this technique of converting something invisible into something we can readily observe is promising.

The ORGAN experiment does not need to be located underground. Instead, it must be cooled to cryogenic temperatures inside a special tool called a dilution refrigerator. Housing the experiment in the fridge and cooling it reduces not only external background light interference but also the thermal radiation given off by all the components in the detector itself.

To stimulate axion-photon conversion, we need a strong magnetic field. Axions interact with the magnetic field and convert into flashes of light. To enable this, our cryogenic setup is fitted with a 12.5 Tesla superconducting solenoid

With the very cold, strong magnetic field in place, reducing the background and stimulating axion-photon conversion, all we need is the detector designed to catch the photons and measure them.

In ORGAN, this detector takes the form of a resonant cavity—essentially a metallic can—which traps the photons that are generated and causes them to “resonate,” or bounce around for a while, thus enhancing our prospects for observing them.

The number of photons inside the resonator is monitored carefully over time, and any spikes above the expected background, and which have the expected signal characteristics, can be attributed to axions.

SABRE South Dark Matter Direct-Detection Experiment :

SABRE South is a dark matter direct-detection experiment [71]. Its goal is to search for a hypothesized type of particle which may constitute dark matter, the mysterious and elusive material that makes up about 23% of the mass-energy of the universe—around five times as much as the matter that we can see.

It will search for WIMPs (Weakly Interacting Massive Particles), one type of candidate dark matter particle.

Unlike previous experiments, this one will be located deep underground in the Stawell Underground Physics Laboratory (SUPL) [72], situated in a cavern in the Stawell Gold Mine in Victoria, Australia. The installation of equipment was begun in October 2023. The heart of the experiment is the detector vessel, which contains sodium-iodide crystals. These crystals are crucial because they are expected to interact with WIMPs. When a WIMP interacts with a sodium-iodide crystal, it produces a burst of light, which is easy to detect.

There are other experiments like CYGNUS [73], ADMX [74], and others. You can check them from the Centre for Dark Matter official website [here](#).

3.3 Indirect Detection experiments :

Fermi Gamma-ray Space Telescope :

The Fermi Gamma-ray Space Telescope [75], launched by NASA in 2008, has made significant contributions to our understanding of the universe, particularly in the study of high-energy phenomena such as gamma rays. The Fermi Gamma-ray Space Telescope, with its two main instruments—the Large Area Telescope (LAT) and the Gamma-ray Burst Monitor [76] (GBM)—is designed to detect gamma rays with unprecedented sensitivity and resolution. Its contributions to dark matter research include :

- **Galactic Center Studies:** The Galactic Center of the Milky Way is a prime location for dark matter searches because it is expected to have a high density of dark matter. The Fermi Telescope has observed an excess of gamma rays from this region [77], which some researchers suggest could be evidence of dark matter annihilation. However, this interpretation is debated, as other astrophysical sources like pulsars might also explain the excess.
- **Dwarf Spheroidal Galaxies:** These small, dark matter-dominated galaxies [78] are considered excellent targets for dark matter searches due to their low background of gamma-ray emission from conventional astrophysical sources. The Fermi Telescope has conducted extensive surveys of these galaxies, placing stringent limits on the properties of dark matter particles.
- **Cosmic Ray Interactions:** The Fermi Telescope also studies gamma rays produced by cosmic rays interacting with interstellar gas and radiation. By understanding these background processes, scientists can better isolate potential signals from dark matter [79].
- **Diffuse Gamma-ray Background:** The Fermi Telescope has mapped the diffuse gamma-ray background [80], the gamma-ray glow that permeates the universe. Analysis of this background can provide clues about the cumulative effect of dark matter annihilation or decay throughout cosmic history.

3.4 Production in colliders :

The Large Hadron Collider (LHC) is one of the powerful tools in high energy physics it allows research into dark matter production [58] [81] through high-energy collisions. This research extends the experimental reach of the Centre to dark matter masses and interactions for which direct detection experiments have less sensitivity, While dark matter particles may not be directly observed in collider experiments, their presence can be inferred indirectly. Collisions at high energies can produce known particles that decay into lighter particles, including potential dark matter candidates. By analyzing the decay products and energy distributions, researchers can search for signatures consistent with dark matter interactions. When dark matter is a stable neutral particle, it can only be generated in pairs during collider experiments. Consequently, the potential for discovery in such searches is constrained by the energy capabilities of the collider. Specifically, the collider's collision energy must exceed twice the mass of the dark matter particle

($\sqrt{s} > 2m_{DM}$) to effectively produce dark matter particles, and of course the LHC with $\sqrt{s} > 13$ Tev is sufficient

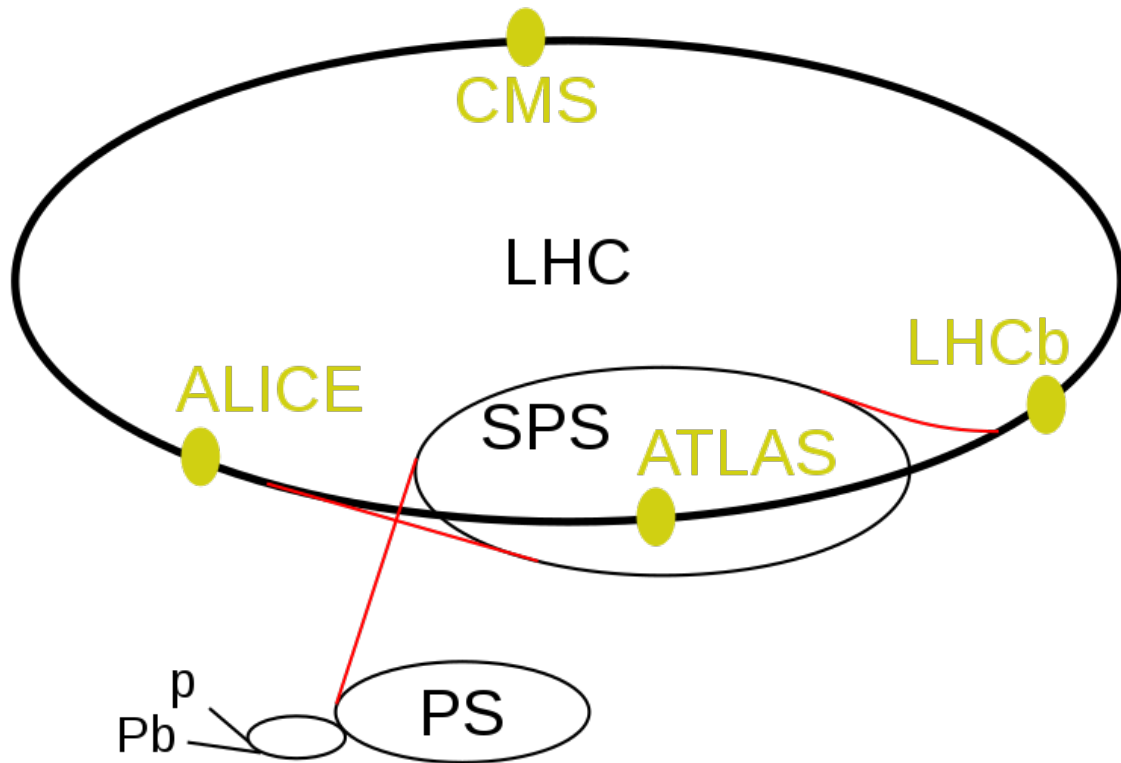


Figure 3.2: The Large Hadron Collider [\[82\]](#)

SPS (Super Proton Synchrotron)

PS (Proton Synchrotron)

DM particles might be detected in the LHC major experiments (detectors) such as ATLAS [\[83\]](#) and CMS [\[84\]](#)

ATLAS (A Toroidal LHC ApparatuS): ATLAS is one of the four major particle detectors at the Large Hadron Collider (LHC) at CERN. It is designed to study a wide range of physics phenomena, including the search for the Higgs boson, the exploration of new particles, and the investigation of fundamental forces and particles that make up the universe.

CMS (Compact Muon Solenoid): CMS is another major particle detector at the LHC, also designed to explore various aspects of particle physics. It has a compact design and focuses on studying phenomena such as the Higgs boson, supersymmetry, and other potential new physics beyond the Standard Model.

Chapter 4

Simulation of Simplified Dark Matter models spin-0/spin-1/spin-2

- **Delphes:** Installation of Delphes can be done by running the command `install Delphes`.
- **Pythia-pgs:** We execute `install pythia-pgs` for installing Pythia-pgs.
- **MadAnalysis5:** To install MadAnalysis5, use the command `install MadAnalysis5`.
- **ExRootAnalysis:** We execute `install ExRootAnalysis` for installing ExRoot-Analysis.
- **MadDM:** For Dark Matter analysis, We will install MadDM by executing `install maddm`.

And this is an example of installation of MadDM

```

e+ mu+ t b t~ b~ z w+ h w- ta- ta+
MG5_aMC>install maddm
  You are installing 'maddm', please cite ref(s): arXiv:1804.00444.
Downloading http://madgraph.phys.ucl.ac.be//Downloads/maddm/maddm_V3.2.13.tar.gz
--2024-03-20 02:06:08-- http://madgraph.phys.ucl.ac.be//Downloads/maddm/maddm_V
3.2.13.tar.gz
Resolving madgraph.phys.ucl.ac.be (madgraph.phys.ucl.ac.be)... 130.104.1.243
Connecting to madgraph.phys.ucl.ac.be (madgraph.phys.ucl.ac.be)|130.104.1.243|:8
0... connected.
HTTP request sent, awaiting response... 200 OK
Length: 604322 (590K) [application/x-gzip]
Saving to: 'maddm.tgz'

maddm.tgz          100%[=====>] 590.16K   155KB/s   in 3.8s

2024-03-20 02:06:12 (154 KB/s) - 'maddm.tgz' saved [604322/604322]

compile maddm. This might take a while.
no compilation needed for plugin. Loading plugin information
Plugin maddm correctly interfaced. Latest official validation for MG5aMC version
 2.9.9.
To use this module, you need to quit MG5aMC and run the executable bin/maddm.py
Installation succeeded
MG5_aMC>

```

Figure 4.2: Packages Installation process in MadGraph.

The latest version of MadDM will automatically be downloaded and installed as a MG5 plug-in

4.3 MadDM :

We mentioned before in packages installation how to install MadDM plugin, We just open the MG5 and write: `MG5_aMC> install maddm`

MadDM needs Python version 2.7 (until now it does not work with python3), SciPy and NumPy

MadDM v.3.2 is a numerical tool to compute dark matter relic abundance, dark matter nucleus scattering rates and dark matter indirect detection predictions in a generic model. The code is based on the existing MadGraph 5 architecture and as such is easily integrable into any MadGraph collider study

MadDM is able to calculate [87] the dark matter relic abundance in models which include a multi-component dark sector, resonance annihilation channels and co-annihilations.

The direct detection [88] module of the MadDM code calculates spin independent / spin dependent dark matter-nucleon cross sections [89] and differential recoil rates as a function of recoil energy, angle and time. The code provides a simplified simulation of detector effects for a wide range of target materials [89] and volumes [87].

The indirect detection module of the MadDM code computes the velocity averaged cross-section for dark matter particles annihilating into n final state particles [90]. It further provides the energy spectra of photons, neutrinos and cosmic-rays generated by these final states after decaying, showering and hadronization. It automatically computes the flux of prompt neutrinos and gamma rays at detection while it provides a user friendly interface with the numerical DRAGON code for obtaining the flux of cosmic rays at Earth [91]. It also provides a user friendly interface with the nested sampling PyMultiNest algorithm for efficient sampling of the model parameter space and allows as well to test the model against the Fermi-LAT dwarf spheroidal galaxy likelihood [90].

4.4 Relic density and Direct Detection of Simplified Dark Matter Model with spin-0 mediator Y_0 :

4.4.1 Fermionic dark matter particles candidate X_d :

These particles are fermions (spin- $\frac{1}{2}$), characterized by possessing a Dirac mass, To generate a simulation for this model with this type of DM you should import the model to the MadDM by the following instruction in this script :

```
#generate
import model DMsimp_s_spin0
define darkmatter xd
generate relic_density
add direct_detection
add indirect_detection
output XD_Y0
```

To get the results we run the following script :

```
#generate
launch XD_Y0
indirect = flux_source
```

```

direct = direct
set sigmav_method madevent
set nevents 30000
set mxd 500 #just an example

```

Relic Density

To find the true relic density we must keep changing in the mass of the candidate and generating new diagrams and this is an example diagram of interaction between X_d and SM particle with the mediator Y_0 in the Fig[4.3]:

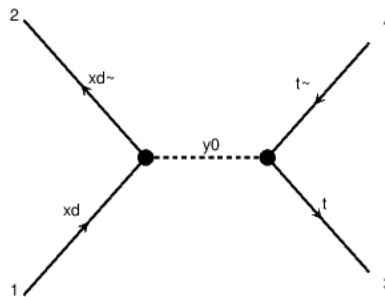


Figure 4.3: Annihilation process of X_d into a pair of top-antitop quarks

we calculated the relic density for this model with different masses and we figured :

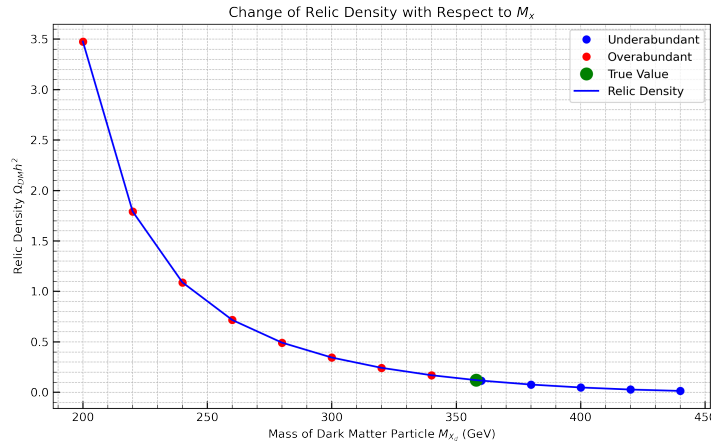


Figure 4.4: The variations of relic density with respect to the mass M_{X_d}

The true value of $\Omega_{DM} h^2 \approx 0.12$ so the mass M_{X_d} corresponding of the true relic density value with approximation is 358 GeV the masses above this value make the relic density overabundant, the masses below this value make the relic density underabundant, the relic density in this particle candidate and this mediator Y_0 inversely proportional with the mass M_{X_d}

Direct Detection :

To run the direct detection simulation `generate direct detection`
This is a Feynmann diagram of collision between up-quark and X_d :

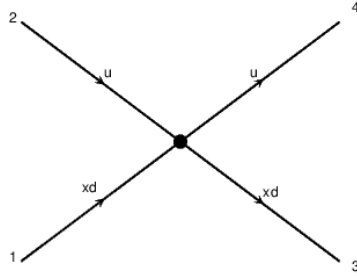


Figure 4.5: Scattering proces $u + X_d = u + X_d$

In direct detection, there are four different experimental methods to calculate the cross-section for collisions with neutrons and protons, considering both cases without and with spin consideration. These cross-sections are calculated for different masses.

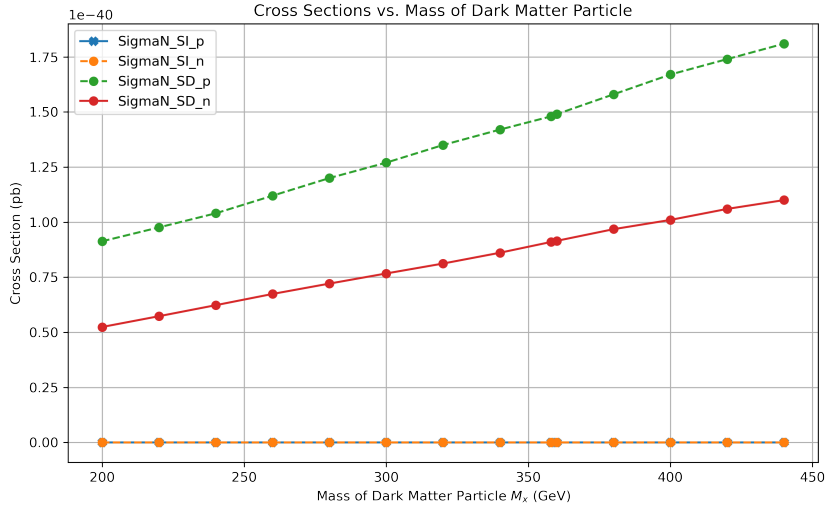
SigmaN SI_p represent the cross section with proton dependent

SigmaN SI_n represent the cross section with neutron dependent

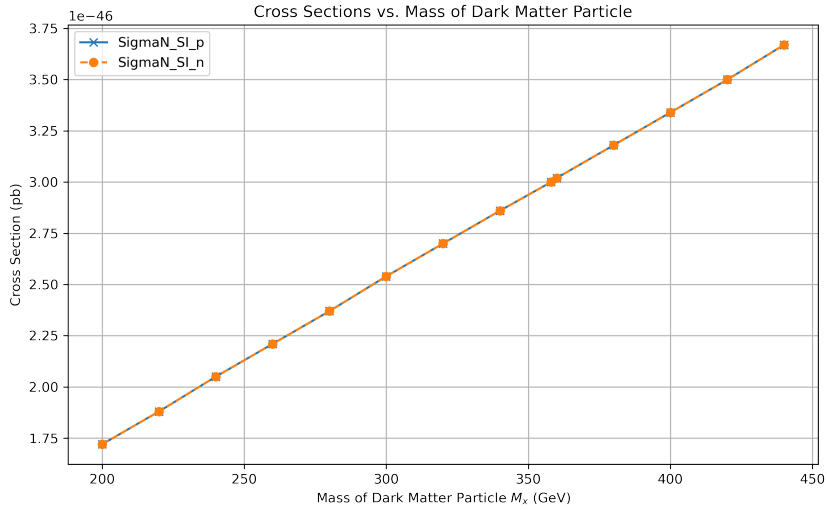
SigmaN SD_p represent the cross section with proton spin dependent

SigmaN SD_n represent the cross section with neutron spin dependant

The "SigmaN SI_p" and "SigmaN SI_n" are identical because the masses of the neutron and the proton are almost equal ($m_p \approx m_n$).



(a) Direct detection Cross-Sections changing with M_{X_d}



(b) Direct detection Cross-Sections spin independent changing with M_{X_d}

Figure 4.6: Comparison of Direct Detection Cross-Sections

From these results, we can conclude:

For the direct detection simulations, the cross-section σ_N for interactions between the dark matter particle and nucleons (protons and neutrons) was calculated. The results demonstrate that the cross-section increases proportionally with the mass of the dark matter particle M_{X_d} . This proportional relationship indicates that heavier dark matter particles have a higher likelihood of interacting with nucleons.

Furthermore, the simulations show that the spin-independent (SI) cross-sections for protons ($\sigma_{SI,p}$) and neutrons ($\sigma_{SI,n}$) are nearly identical. This similarity arises because the masses of the proton and neutron are almost equal ($m_p \approx m_n$), leading to comparable interaction probabilities for the dark matter particle with both types of nucleons. The spin-dependent (SD) cross-sections, however, were calculated separately for protons and neutrons, reflecting the different interaction dynamics when considering

the spin of the nucleons. In summary, these simulations underscore the importance of the dark matter particle mass in determining relic density and direct detection cross-sections. The proportional increase in cross-section with mass and the near-identical nature of the spin-independent cross-sections for protons and neutrons provide valuable insights into the interactions of dark matter particles with ordinary matter, guiding experimental searches and theoretical models in the quest to understand dark matter.

4.4.2 Real Scalar Dark Matter particles candidate X_r :

X_r dark matter particles are real scalar particles. Unlike fermionic dark matter particles, real scalar dark matter particles have spin 0 (Bosons) and are described by a single real-valued field (like the Klein-Gordon field)

In the case of this DM type to run the simulation we will change the instruction of "define darkmatter xd" with "define darkmatter xr" and run the simulation with the same previous steps either in the relic density or the indirect detection

Relic Density :

Feynmann diagram of a relic density calculations :

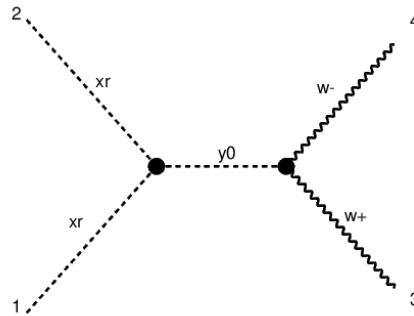


Figure 4.7: Annihilation process of X_r into W^+ and W^-

We calculated the relic density for this model with different masses and we figured :

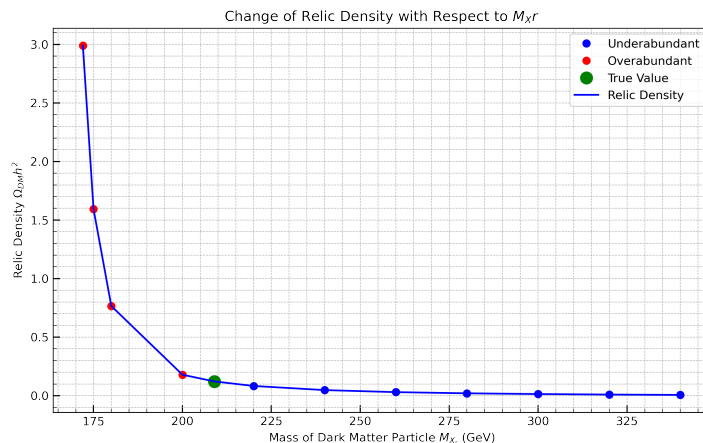


Figure 4.8: variations of DM scalar type's relic density with respect to mass M_{X_r} .

Unlike the previous type the true value of the relic density is smaller it is 209 GeV as shown in the Fig4.8

The relic density $\Omega_{DM}h^2$ is found to be inversely proportional to the mass M_{X_r} . As the mass of the dark matter particle increases, the relic density decreases, and vice versa. This relationship is crucial in determining the viable mass range for the dark matter particle that aligns with the observed relic density value of $\Omega_{DM}h^2 \approx 0.12$. For this model, the mass M_{X_r} corresponding to the observed relic density is approximately 209 GeV. Masses significantly above this value result in an overabundant relic density, while masses significantly below it lead to an underabundant relic density.

Direct Detection :

this is an example of direct detection proces :

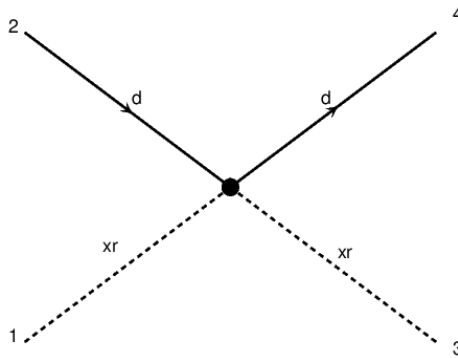
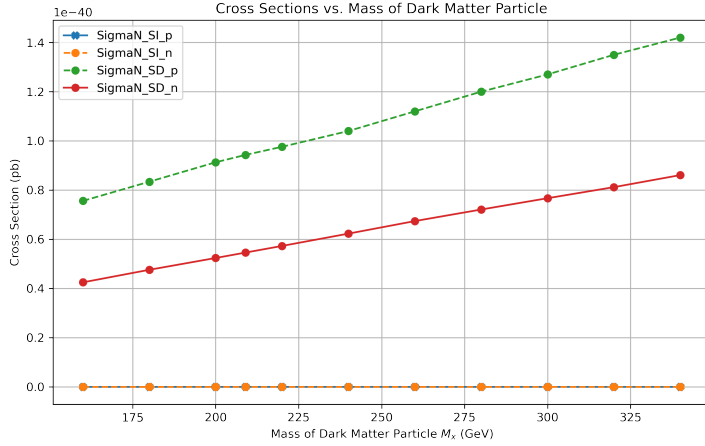
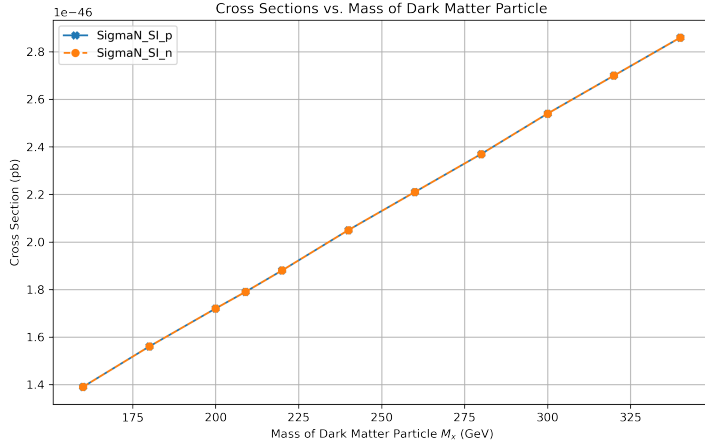


Figure 4.9: Scattering process between down-quark and X_r

The direct detection of this model the results looks the same in the identical masses of X_d and X_r as shown in Fig4.10b



(a) Direct detection Cross-Sections changing with M_{X_r}



(b) Direct detection Cross-Sections SI changing with M_{X_r}

Figure 4.10: Comparison of Direct Detection Cross-Sections for M_{X_r}

4.4.3 Complex scalar dark matter particles candidate X_c :

Complex dark matter, denoted as X_c refers to dark matter particles that are complex scalars. These particles have properties similar to real scalar dark matter but are described by complex-valued fields instead of real-valued fields. The term "complex" here refers to the mathematical representation of the particle, not necessarily implying that the particle is electrically charged.

Key Points About Complex Dark Matter (X_c):

- **Complex Scalar Field:** Unlike real scalar dark matter particles, which are represented by a single real field, complex scalar dark matter particles are represented by a complex field. This means the field has both a real and an imaginary component.
- **Charge and Interactions : Electric Charge :** Complex scalar dark matter particles can be neutral or carry a non-electric charge. When discussing dark matter, the particles are usually assumed to be electrically neutral to avoid rapid decay or

interaction with electromagnetic forces, which would make them incompatible with observations of dark matter being non-luminous.

Other Charges : They might carry other types of "charges" such as a charge under a hidden sector gauge group or a conserved quantum number like dark charge or baryon number, which does not directly interact with Standard Model particles.

- **Annihilation and Interactions:** Just like real scalar dark matter, complex dark matter particles can annihilate into Standard Model particles through interactions mediated by Y_0 boson.

The presence of a complex field allows for richer interactions and potential symmetries in the model, which can affect the phenomenology of dark matter.

- **Stability:** Complex dark matter particles are usually assumed to be stable, meaning they do not decay into other particles over cosmological timescales. This stability is often guaranteed by imposing a symmetry such as a $U(1)$ symmetry, which results in a conserved quantum number.

- **Example Process :** $X_c + \bar{X}_c \rightarrow Y_0 \rightarrow \text{SM particles}$ for example into to higgs

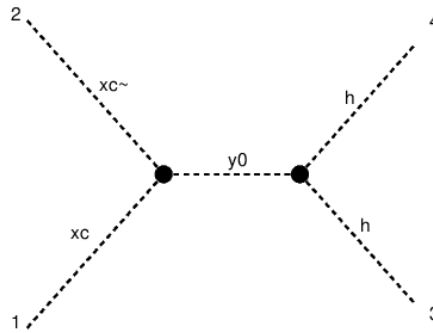


Figure 4.11: Annihilation process of X_c particles into pair of two higgs bosons

In conclusion complex dark matter refers to particles described by complex scalar fields. These particles can be neutral or carry non-electric charges under new symmetries or hidden sector interactions. They interact through mediators, allowing them to annihilate into Standard Model particles while remaining consistent with dark matter's non-luminous and weakly interacting nature.

Relic Density :

The instruction of choosing this type of DM is " `Define darkmatter xc` " while we continue using the same instructions

The calculation of the relic density with different mass values give us the following results :

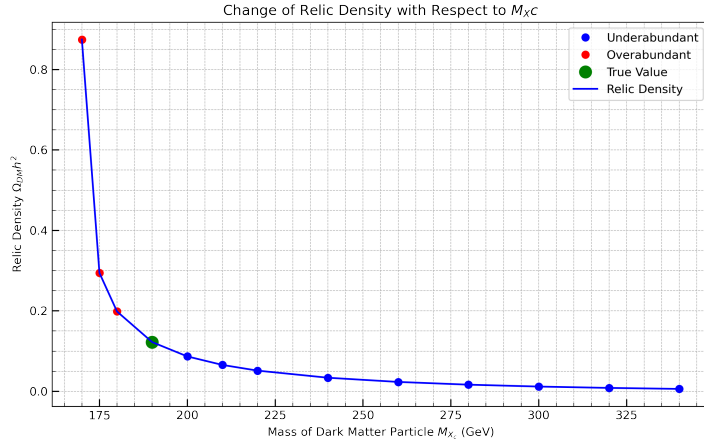


Figure 4.12: The variations of relic density with respect to M_{X_c}

As shown in the Figure [4.12](#) the value corresponding to experimental results is 190 GeV, Like the other two types their relic density is inversely proportional to the mass M_{X_c}

Direct Detection :

This is an example of direct detection process of complex scalar DM candidate :

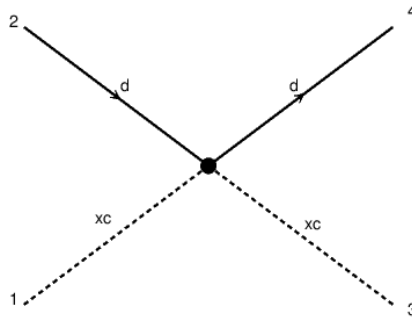
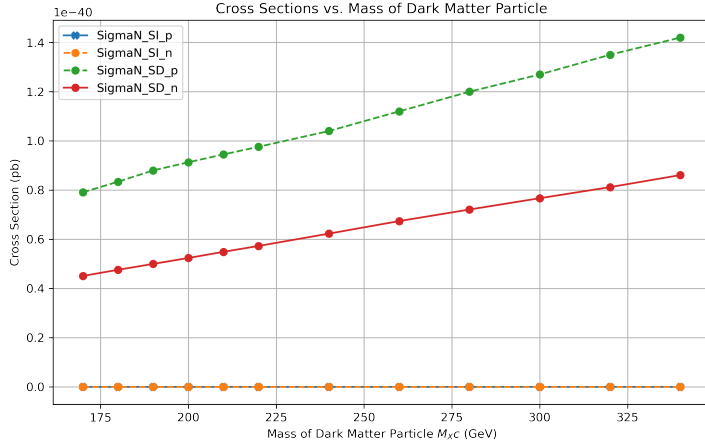
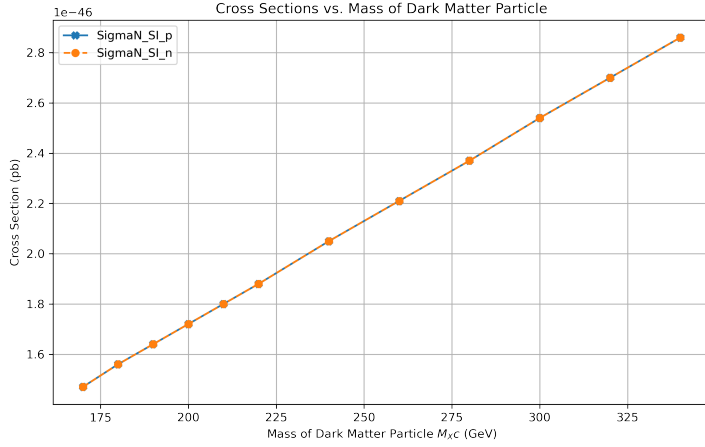


Figure 4.13: Scattering process between down-quark and X_c

the result in this type of DM looks the same with the other types as shown in the figure below :



(a) Direct detection Cross-Sections SI/SD changing with M_{X_c}



(b) Direct detection Cross-Sections SI changing with M_{X_r}

Figure 4.14: Comparison of Direct Detection Cross-Sections for M_{X_c}

Direct Detection Discussion :

For direct detection experiments, we calculated the spin-independent (SI) and spin-dependent (SD) cross-sections for interactions with protons and neutrons. Our findings show:

- The spin-independent cross-sections for both protons (σ_{SI_p}) and neutrons (σ_{SI_n}) are identical across all three types of dark matter particles. This is due to the similar masses and interaction properties of protons and neutrons.
- The spin-dependent cross-sections (σ_{SD_p} and σ_{SD_n}) vary more significantly but still show similar trends in their dependence on dark matter mass.

Despite the different spin properties of X_d , X_r , and X_c , the direct detection cross-sections for SI interactions are remarkably similar. This is because the SI interactions are primarily governed by the scalar couplings, which do not depend strongly on the spin of the dark matter particle.

4.5 Relic density of Simplified Dark matter model with spin-1 mediator Y_1^μ

This model is like other simplified models but with vector mediator spin-1 and possibility of coupling with leptons, this one has two candidates X_d and X_r

4.5.1 Fermionic dark matter particles candidate X_d :

The calculation of the relic density with different mass values give us the following results :

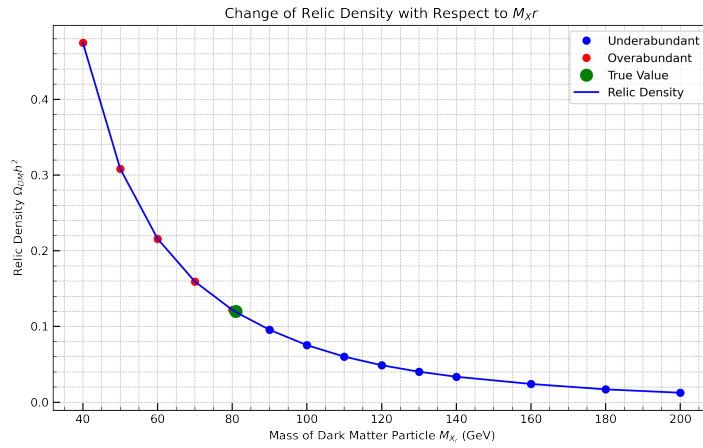


Figure 4.15: The variations of Relic density with respect to M_{X_d}

As shown in the Figure 4.15 the value corresponding to experimental results is 81 GeV

4.5.2 Complex Scalar dark matter particles candidate X_c :

For the complex DM candidates the relic density is :

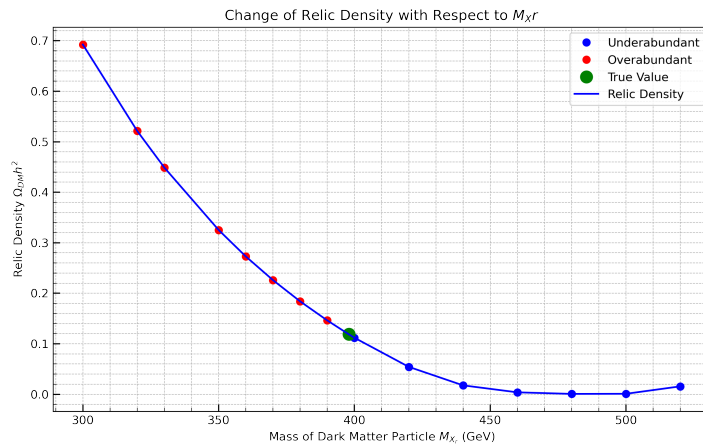


Figure 4.16: The variations of Relic density with respect to M_{X_c}

As shown in the Figure 4.16 the value corresponding to experimental results is 398 GeV

4.6 Relic density of Simplified Dark matter model spin-2 mediator $Y_2^{\mu\nu}$

This model associated with a spin-2 like graviton and there are three different types of candidates X_r and X_d like the previous models and X_v the new one candidate with spin-1 we called it vector DM

4.6.1 Fermionic dark matter particles candidate X_d :

The calculation of the relic density with different mass values give us the following results :

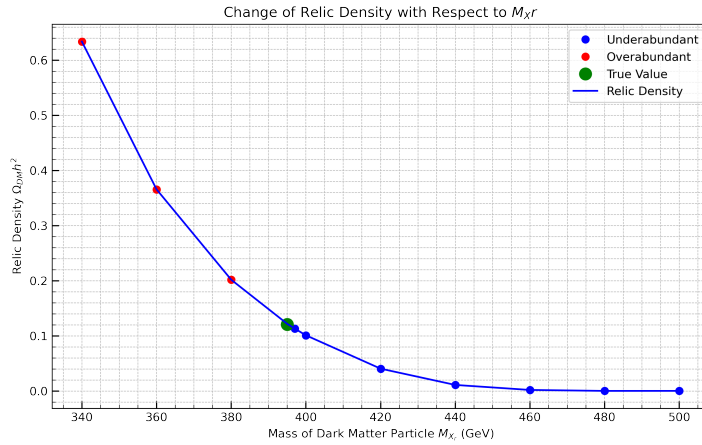


Figure 4.17: The variations of Relic density with respect to M_{X_d}

As shown in the Figure the mass value corresponding to experimental results is 398 GeV

4.6.2 Real Scalar Dark matter particles candidate X_r :

the calculation of the relic density with different mass values give us the following results :

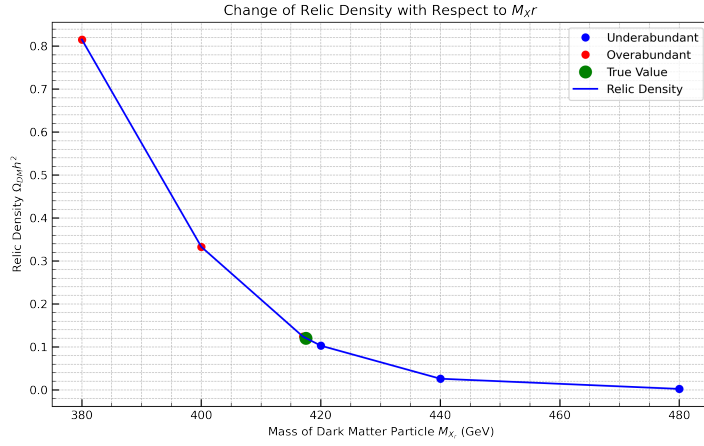


Figure 4.18: Variations of Relic density with respect to MX_R

As shown in the Figure the value corresponding to experimental results is 417 GeV

4.6.3 Vector Dark matter particles candidate X_v :

The calculation of the relic density with different mass values give us the following results :

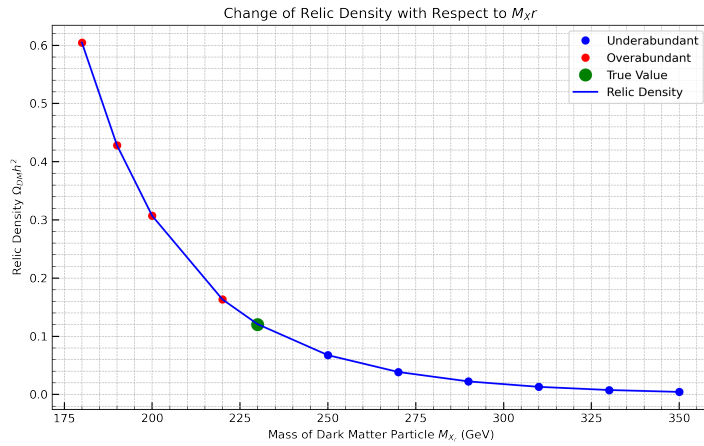


Figure 4.19: Variations of Relic density with respect to MX_V

As shown in the Figure 4.19 the value corresponding to experimental results is 230 GeV

4.6.4 Discussion :

In conclusion we can summarize the results in the next table [4.1](#):

Table 4.1: Mass values for true relic density ($\Omega_{DM}h^2 \approx 0.12$) for different DM candidates of SDMMs

Mediator Model	Dark Matter Particle	Mass (GeV)
Y_0	X_D	358
	X_R	209
	X_C	190
Y_1	X_D	81
	X_C	398
Y_2	X_D	395
	X_V	230
	X_R	417

The relic density ($\Omega_{DM}h^2$) of dark matter particles is inversely proportional to their masses. For the Y_0 mediator model, we have calculated the relic density for each type of particle and identified the mass values corresponding to the true relic density value ($\Omega_{DM}h^2 \approx 0.12$). For X_d , the true relic density is achieved at a mass of approximately 358 GeV. For X_r , the true relic density is achieved at a mass of approximately 209 GeV. For X_c , the true relic density is achieved at a mass of approximately 190 GeV.

Despite their differences in spin and nature (fermionic versus scalar), the behavior of relic density as a function of mass shows a similar trend: higher mass values result in lower relic density, and vice versa. This is because the annihilation cross-section, which determines how efficiently dark matter particles annihilate in the early universe, generally increases with the mass of the dark matter particle. As a result, heavier particles annihilate more efficiently, leaving a smaller relic density.

Our analysis reveals that the variations in relic density with respect to mass, as well as the direct detection cross-sections, exhibit similar behaviors for different types of dark matter particles (X_d , X_r , and X_c), despite their differing spins. The true relic density is achieved at different mass values for each type of particle in the Y_0 mediator model: 358 GeV for X_d , 209 GeV for X_r , and 190 GeV for X_c . The identical behavior in spin-independent cross-sections across different dark matter particles highlights the universality of scalar interactions in direct detection experiments. This suggests that while the nature of the dark matter particle (fermionic versus scalar) affects the specific mass values for relic density, the underlying interaction mechanisms in direct detection remain consistent, leading to similar experimental signatures.

Additionally, for other mediator models, we observe varying mass values corresponding to the true relic density. In the Y_1 mediator model, the true relic density is achieved at a mass of 81 GeV for X_d and 398 GeV for X_c . This variation indicates that the interaction specifics of the Y_1 mediator influence the annihilation cross-sections differently compared to the Y_0 model, leading to different mass values for achieving the same relic density. For the Y_2 mediator model, the true relic density is reached at 395 GeV for X_d , 230 GeV for X_v , and 417 GeV for X_R . This further highlights how different mediators can affect the required mass values to achieve the observed relic density, while the overall trend of higher mass leading to lower relic density remains consistent.

We did not calculate the direct detection cross-sections for the Y_1 and Y_2 mediator

models because it was found that these cross-sections are the same across different mediator models. Direct detection primarily depends on the mass and the velocity (momentum) of the dark matter particles rather than the specifics of the mediator model. This consistency underscores the importance of mass and velocity in determining direct detection cross-sections, ensuring that the experimental signatures remain similar despite differences in the mediator models. The varying mass values across different mediator models underscore the importance of considering different mediator scenarios when studying dark matter properties and their implications for both relic density and direct detection experiments.

Chapter 5

Simulation of Dark Matter production in Colliders

5.1 Introduction :

At the LHC, protons are accelerated towards each other for head-on collisions, resulting in net momentum along the beamline but none in the transverse direction. Missing transverse energy (MET) is calculated as the momentum vector sum of all recorded particles in the transverse plane. Nonzero MET indicates an escaping particle, potentially a neutrino or an exotic particle like dark matter candidate, in this chapter we are going to simulate missing transverse energy in the detector of the dark matter particles produced in the proton proton collision. In our simulation we focus on monojet technique used at the LHC to search for dark matter. It relies on the possibility that quark-antiquark interactions could produce dark matter candidates in addition to a monojet produced in the initial state radiation, like weakly interacting massive particles (WIMPs). These particles would likely pass through the detector without interacting, similar to neutrinos. In this simulation we will consider all the simplified models already discussed in the previous chapter.

5.2 Simplified Dark matter model spin-0 mediator Y_0

In the proton-proton $\sqrt{s} = 13\text{TeV}$ collision simulation we will produce the DM particles with different masses, in this model we can produce DM particles through the $b\bar{b}$ annihilation.

```
#generate
import model DMsimp_s_spin0
define darkmatter xd
define q = p / g
generate q q > y0 > xd xd~ j
output XD_Y0
launch
```

We set the dark matter mass 358 GeV for the X_d type and choose Pythia8 generator [92] for hadronization

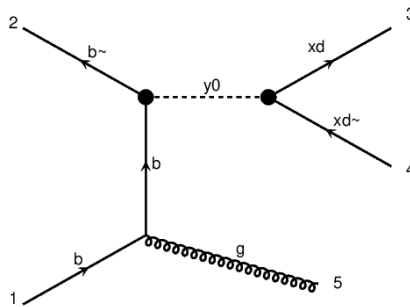


Figure 5.1: The process $b\bar{b} \rightarrow y_0 \rightarrow xd + \bar{x}d + jet$

We follow the same steps with X_r and X_c with masses 209 GeV and 190 GeV respectively and we simulate the transverse missing energy (MET) then we plot our results using Rivet [93] [94] data analysis, Our (MET) results are in Fig 5.2 :

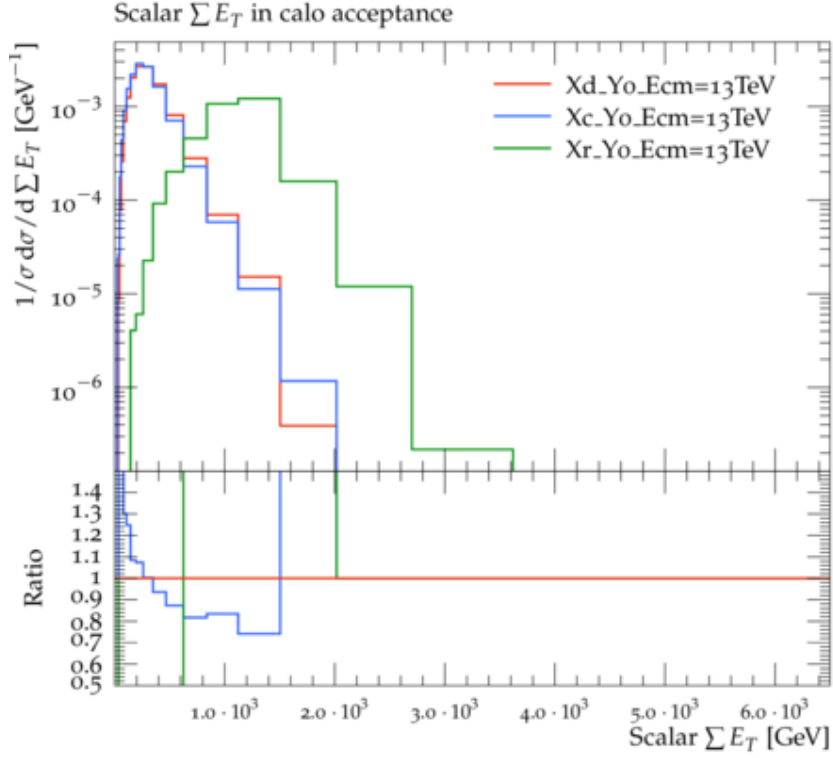


Figure 5.2: MET of DM in spin-0

5.3 Simplified Dark matter model spin-1 mediator Y_1^μ

To simulate this Simplified DM we need to import it

```
import model DMsimp_s_spin1
```

We set the DM mass at 81 GeV for the X_d type and choose Pythia8 generator for hadronization

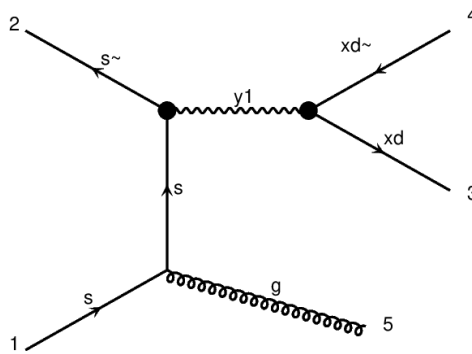


Figure 5.3: The process $q\bar{q} \rightarrow Y_0 \rightarrow X_d + \bar{X}_d + jet$

We follow the same steps for DM particle X_c at the mass of 398 GeV and we calculate the transverse missing energy (MET) using Rivet and plot the results in the Fig [5.4](#)

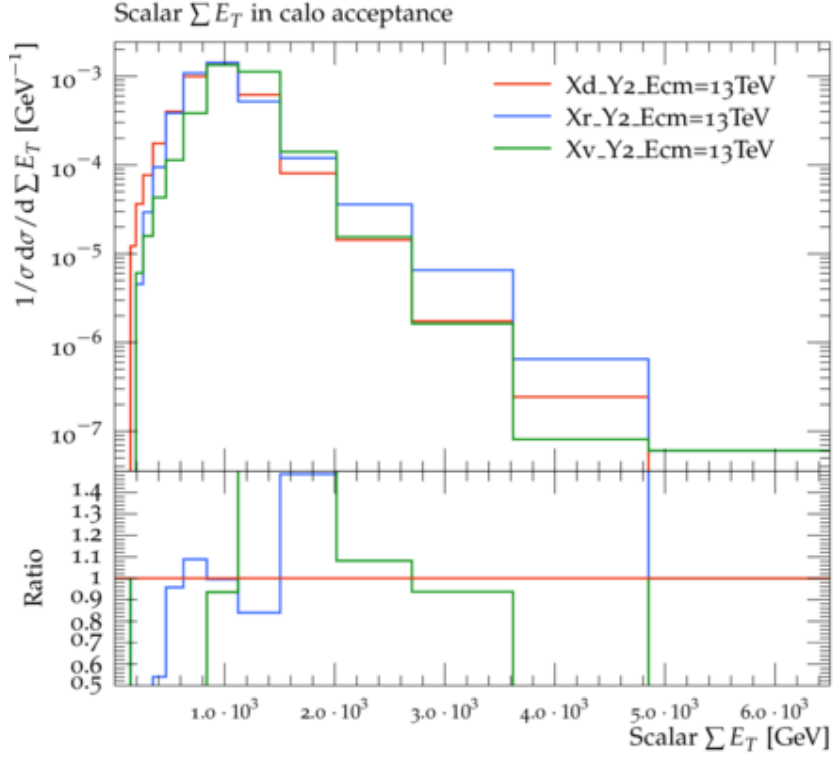


Figure 5.6: MET of DM in spin-2

5.5 Neutrinos missing energy :

We use the missing transverse energy (MET) to measure non-interacting particles like Neutrinos, we use the MET analysis of the neutrinos as test for our dark matter MET analysis

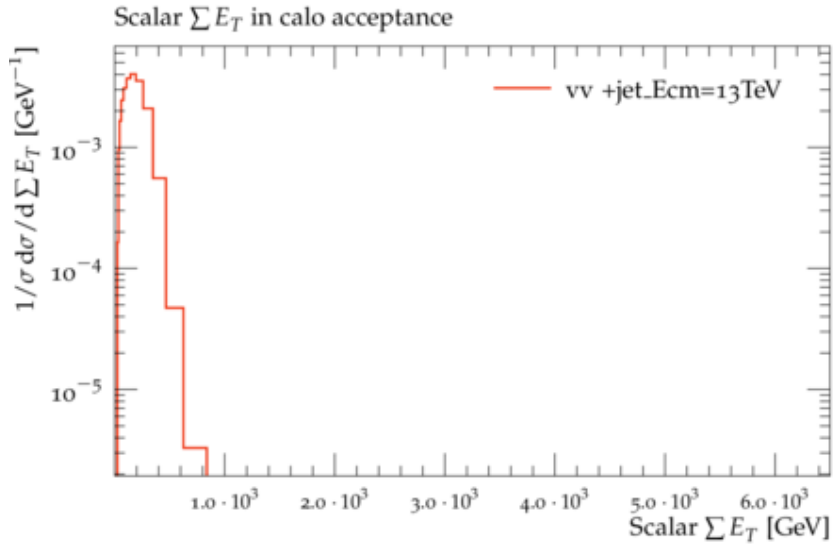


Figure 5.7: Missing Energy of SM's neutrinos

The y-axis of the plot represents $\frac{1}{\sigma} \frac{d\sigma}{d\Sigma E_T}$ in units of GeV^{-1} , which is the normalized differential cross-section with respect to the scalar sum of transverse energy, while the

x-axis represents the scalar sum of transverse energy (ΣE_T) in GeV. The plot shows a steep drop-off in the differential cross-section as ΣE_T increases. Most of the events are concentrated at lower values of ΣE_T , indicating that the majority of neutrino events result in lower missing transverse energy.

The majority of events have low ΣE_T , consistent with the production of neutrinos from lower energy processes, such as the decay of W and Z bosons. These processes typically produce softer missing energy signatures. There are very few events with high ΣE_T , indicating that high missing energy events are rare in the Standard Model when only neutrinos are considered. This is expected as neutrinos from SM processes usually do not carry away large amounts of transverse energy compared to hypothetical heavy dark matter particles.

Low ΣE_T : The majority of events have low ΣE_T , consistent with the production of neutrinos from lower energy processes, such as the decay of W and Z bosons. These processes typically produce softer missing energy signatures. High ΣE_T : There are very few events with high ΣE_T , indicating that high missing energy events are rare in the Standard Model when only neutrinos are considered. This is expected as neutrinos from SM processes usually do not carry away large amounts of transverse energy compared to hypothetical heavy dark matter particles.

5.6 Discussion :

Here is a detailed comparison of these results:

5.6.1 Spin-0 Mediator Y_0

The model details include DM particle masses of X_d (358 GeV), X_r (209 GeV), and X_c (190 GeV). The process considered is $q\bar{q} \rightarrow Y_0 \rightarrow X + \bar{X} + j$. The missing energy distribution is relatively broad, indicating a wide range of E_T^{miss} . The distribution peaks at lower E_T^{miss} values, which reflects the masses of the produced DM particles.

5.6.2 Spin-1 Mediator Y_1^μ

The model details include DM particle masses of X_d (81 GeV) and X_c (398 GeV). The process considered is $q\bar{q} \rightarrow Y_1 \rightarrow X + \bar{X} + j$. The missing energy distribution shows a sharp peak, suggesting a more distinct production mechanism with a specific energy range. The distribution is less broad compared to the spin-0 mediator, indicating a more constrained kinematic space.

5.6.3 Spin-2 Mediator $Y_2^{\mu\nu}$

The model details include DM particle masses of X_d (395 GeV), X_r (417 GeV), and X_v (230 GeV). The process considered is $q\bar{q} \rightarrow Y_2 \rightarrow X + \bar{X} + j$. The missing energy distribution shows wide peaks, with higher values of E_T^{miss} being more probable, reflecting the higher masses of the DM particles involved.

5.6.4 Comparison with Neutrinos in the SM

The missing energy distribution for neutrinos in the SM shows a steep drop-off with most events at lower E_T^{miss} . High E_T^{miss} events are rare, corresponding to lower energy scales of SM processes.

In general and compared to neutrinos the MET plots for dark matter models has a large tail at high energy values, This is mostly due to the presence of the potential weakly interacting massive dark matter particles WIMPS in the event , it is also might be due to mismeasurments of monojet energies, which may show up as a fake missing energy. The search for dark matter continues, with the LHC contributing valuable insights.

5.7 Conclusion

The comprehensive exploration of dark matter in this study illuminates several key findings that collectively advance our understanding of this elusive phenomenon. Historical observations, notably by Fritz Zwicky and Vera Rubin, highlighted gravitational anomalies in galaxy clusters and rotation curves that could not be explained by visible matter alone, suggesting the existence of dark matter. Further empirical support for dark matter comes from phenomena like gravitational lensing and cosmic microwave background (CMB) fluctuations, which underscore its critical role in cosmic structure formation and evolution. Within the Λ CDM framework, dark matter is indispensable for explaining the universe's large-scale structure and dynamics. Despite extensive research, the precise nature of dark matter remains unidentified.

Theoretical models propose various candidates such as Weakly Interacting Massive Particles (WIMPs), axions, and sterile neutrinos, yet no direct detections have been confirmed. Detection strategies include direct detection experiments like XENON1T and LUX-ZEPLIN, which aim to observe dark matter interactions with ordinary matter through nuclear recoils, and indirect detection methods that seek signals from dark matter annihilation or decay, with no conclusive evidence yet observed. Collider experiments at facilities like the Large Hadron Collider (LHC) attempt to produce dark matter particles, but have not observed missing energy signatures consistent with such production.

Additionally, simplified dark matter models with different spin mediators (spin-0, spin-1, and spin-2) have been employed to simulate potential interactions and relic densities, offering critical insights into the characteristics and detectability of dark matter particles. These efforts continue to refine the range of viable dark matter properties and guide future experimental searches. The challenges faced highlight the complexity of detecting dark matter, yet advancements in detector sensitivity, theoretical models, and complementary detection methods hold promise for future breakthroughs. The integration of diverse detection strategies and theoretical innovations remains vital in resolving the dark matter enigma, with profound implications for our understanding of the universe and potential new physics beyond the Standard Model.

Bibliography

- [1] F. Zwicky, “Dark matter in the coma cluster,” *Astrophysical Journal*, vol. 86, no. 2, pp. 217–246, 1937.
- [2] E. Bertschinger, *Dark matter cosmology*, <http://ned.ipac.caltech.edu/level5/ESSAYS/Bertschinger/bertschinger.html>, Retrieved 30 May 2014, 2014.
- [3] M.-C. Anisiu, “Vera rubin and the hypothesis of dark matter existence,” vol. 36, pp. 13–23, Jan. 2018.
- [4] B. P. Dolan, *Einstein’s General Theory of Relativity: A Concise Introduction*. Cambridge University Press, 2023.
- [5] J. Newby, *Galaxy rotation curve*, Accessed: 2024-07-01, 2019. [Online]. Available: <https://sites.temple.edu/profnewby/2019/05/04/galaxy-rotation-curve/>.
- [6] B. A. Robson, “Introductory chapter: Standard model of cosmology,” in *Redefining Standard Model Cosmology*, B. A. Robson, Ed., Rijeka: IntechOpen, 2019, ch. 1. DOI: [10.5772/intechopen.85605](https://doi.org/10.5772/intechopen.85605). [Online]. Available: <https://doi.org/10.5772/intechopen.85605>.
- [7] A. G. Doroshkevich and I. D. Novikov, “Mean radiation density in metagalaxy and some problems of relativistic cosmology,” *Doklady Akademii Nauk SSSR*, vol. 154, no. 4, pp. 809–811, 1964. [Online]. Available: <http://mi.mathnet.ru/dan29125>.
- [8] S. Panda, “Gravitational lensing - a short treatise,” Apr. 2016.
- [9] R. S. Ellis, “Gravitational lensing: A unique probe of dark matter and dark energy,” *Philosophical Transactions of the Royal Society A: Mathematical, Physical and Engineering Sciences*, vol. 368, no. 1914, pp. 967–987, 2010. DOI: [10.1098/rsta.2009.0209](https://doi.org/10.1098/rsta.2009.0209).
- [10] S. Panda, “Gravitational lensing - a short treatise,” Apr. 2016.
- [11] J. R. Primack, *Dark matter and large-scale structure*, Santa Cruz Institute for Particle Physics, University of California, Unpublished work, Santa Cruz, CA 95064, unknown. [Online]. Available: <https://www.slac.stanford.edu/econf/C940808/pdf/ssi94-006.pdf>.
- [12] Harvard-Smithsonian Center for Astrophysics, *Large-scale structure*, 2024. [Online]. Available: <https://www.cfa.harvard.edu/research/topic/large-scale-structure>.
- [13] D. H. Hartmann and B. S. Meyer, *Nucleosynthesis*, AccessScience, Retrieved June 10, 2024, from <https://doi.org/10.1036/1097-8542.461110>, Aug. 2021. [Online]. Available: <https://www.accessscience.com/content/article/a461110>.
- [14] Chandra X-ray Observatory, *Dark universe*, 2024. [Online]. Available: <https://chandra.harvard.edu/darkuniverse/>.

- [15] NASA WMAP Science Team, *Wilkinson microwave anisotropy probe (wmap): Nine-year data*, 2006. [Online]. Available: <https://map.gsfc.nasa.gov/media/060915/index.html>.
- [16] M. Milgrom, “A Modification of the Newtonian Dynamics as a Possible Alternative to the Hidden Mass Hypothesis,” vol. 270, pp. 365–370, Jul. 1983. DOI: [10.1086/161130](https://doi.org/10.1086/161130).
- [17] X. Hernandez, “Internal kinematics of gaia dr3 wide binaries: Anomalous behaviour in the low acceleration regime,” *arXiv preprint arXiv:2304.07322*, 2023. [Online]. Available: <https://arxiv.org/pdf/2304.07322>.
- [18] C. Pittordis and W. Sutherland, “Wide binaries from gaiaedr3: Preference for gr over mond?” *Open Journal of Astrophysics*, vol. 3, p. 15, 2023, Accepted on January 31, 2023; original submission on July 13, 2022. [Online]. Available: <https://arxiv.org/pdf/2205.02846>.
- [19] I. Banik, C. Pittordis, W. Sutherland, *et al.*, “Strong constraints on the gravitational law from Gaia DR3 wide binaries,” *Monthly Notices of the Royal Astronomical Society*, vol. 527, no. 3, pp. 4573–4615, Nov. 2023.
- [20] A. D. Dolgov, “Massive Primordial Black Holes,” *PoS*, vol. MULTIF2019, p. 013, 2020. DOI: [10.22323/1.362.0013](https://doi.org/10.22323/1.362.0013). arXiv: [1911.02382](https://arxiv.org/abs/1911.02382) [astro-ph.CO].
- [21] C. A. Nelson *et al.*, “The MACHO Project HST Follow-Up: The Large Magellanic Cloud Microlensing Source Stars,” Feb. 2009. arXiv: [0902.2213](https://arxiv.org/abs/0902.2213) [astro-ph.GA].
- [22] K. Griest, “Baryonic dark matter and Machos,” *Nucl. Phys. B Proc. Suppl.*, vol. 91, J. Law, R. W. Ollerhead, and J. J. Simpson, Eds., pp. 393–397, 2001. DOI: [10.1016/S0920-5632\(00\)00967-1](https://doi.org/10.1016/S0920-5632(00)00967-1).
- [23] P. Popowski *et al.*, “Microlensing optical depth towards the galactic bulge using clump giants from the MACHO survey,” *Astrophys. J.*, vol. 631, pp. 879–905, 2005. DOI: [10.1086/432246](https://doi.org/10.1086/432246). arXiv: [astro-ph/0410319](https://arxiv.org/abs/astro-ph/0410319).
- [24] J. Calcino, J. Garcia-Bellido, and T. M. Davis, “Updating the MACHO fraction of the Milky Way dark halowith improved mass models,” *Mon. Not. Roy. Astron. Soc.*, vol. 479, no. 3, pp. 2889–2905, 2018. DOI: [10.1093/mnras/sty1368](https://doi.org/10.1093/mnras/sty1368). arXiv: [1803.09205](https://arxiv.org/abs/1803.09205) [astro-ph.CO].
- [25] *Particle Dark Matter: Observations, Models and Searches*. Cambridge University Press, 2010.
- [26] D. J. E. Marsh, D. Ellis, and V. M. Mehta, *Dark Matter: Evidence, Theory, and Constraints*. Princeton University Press, Sep. 2024, ISBN: 978-0-691-24952-0.
- [27] G. Gelmini, “Detecting weakly interacting massive particles,” *Reports on Progress in Physics*, vol. 80, Jun. 2017. DOI: [10.1088/1361-6633/aa6e5c](https://doi.org/10.1088/1361-6633/aa6e5c).
- [28] G. Belanger, F. Boudjema, C. Hugonie, A. Pukhov, and A. Semenov, “Relic density of dark matter in the next-to-minimal supersymmetric standard model,” *Journal of Cosmology and Astroparticle Physics*, vol. 2005, no. 09, p. 001, 2005.
- [29] G. Busoni, A. De Simone, T. Jacques, E. Morgante, and A. Riotto, “Making the most of the relic density for dark matter searches at the lhc 14 tev run,” *arXiv preprint arXiv:1410.7409*, 2014. [Online]. Available: <https://arxiv.org/abs/1410.7409>.

- [30] R. Higuchi, S. Iguro, S. Okawa, and Y. Omura, “Light mass window of inert doublet dark matter with lepton portal interaction,” *Phys. Rev. D*, vol. 109, no. 7, p. 075 007, 2024. DOI: [10.1103/PhysRevD.109.075007](https://doi.org/10.1103/PhysRevD.109.075007). arXiv: [2310.13685 \[hep-ph\]](https://arxiv.org/abs/2310.13685).
- [31] S. Banerjee, F. Boudjema, N. Chakrabarty, and H. Sun, “Relic density of dark matter in the inert doublet model beyond leading order for the low mass region. ii. coannihilation,” *Phys. Rev. D*, vol. 104, p. 075 003, 7 Oct. 2021. DOI: [10.1103/PhysRevD.104.075003](https://doi.org/10.1103/PhysRevD.104.075003). [Online]. Available: <https://link.aps.org/doi/10.1103/PhysRevD.104.075003>.
- [32] F. Danielsson and M. Mäkelä, *A study on the relic abundance of dark matter using the boltzmann equation*, SA114X Degree Project in Engineering Physics, First Level, Department of Physics, KTH Royal Institute of Technology, Supervisor: Mattias Blennow, 2019. [Online]. Available: <https://www.diva-portal.org/smash/get/diva2:1341326/FULLTEXT01.pdf>.
- [33] M. Backović, K. Kong, and M. McCaskey, “Maddm v.1.0: Computation of dark matter relic abundance using madgraph 5,” *Physics of the Dark Universe*, vol. 5-6, pp. 18–28, 2014, Hunt for Dark Matter, ISSN: 2212-6864. DOI: <https://doi.org/10.1016/j.dark.2014.04.001>. [Online]. Available: <https://www.sciencedirect.com/science/article/pii/S2212686414000107>.
- [34] R. J. Gaitskell, “Direct detection of dark matter,” *Annu. Rev. Nucl. Part. Sci.*, vol. 54, pp. 315–359, 2004.
- [35] E. S. Yeung, “Indirect detection methods: Looking for what is not there,” *Accounts of Chemical Research*, vol. 22, no. 4, pp. 125–130, 1989.
- [36] T. R. Slatyer, “Indirect detection of dark matter,” *Theoretical Advanced Study Institute in Elementary Particle Physics: anticipating the next discoveries in particle physics*, pp. 297–353, 2018.
- [37] ATLAS Collaboration, *ATLAS-PHOTO-2019-013-7*, 2019. [Online]. Available: <https://cds.cern.ch/images/ATLAS-PHOTO-2019-013-7>.
- [38] M. K. Gaillard, P. D. Grannis, and F. J. Sciulli, “The standard model of particle physics,” *Reviews of Modern Physics*, vol. 71, no. 2, S96, 1999.
- [39] I. Brivio and M. Trott, “The standard model as an effective field theory,” *Physics Reports*, vol. 793, pp. 1–98, 2019.
- [40] S. Weinberg, *The quantum theory of fields*. Cambridge university press, 1995, vol. 2.
- [41] A. H. Chamseddine and A. Connes, “Why the standard model,” *Journal of Geometry and Physics*, vol. 58, no. 1, pp. 38–47, 2008.
- [42] S. F. Novaes, “Standard model: An introduction,” *10th Jorge Andre Swieca Summer School: Particle and Fields*, pp. 5–102, 2000.
- [43] K. Riesselmann, “Limitations of a standard model higgs boson,” *arXiv preprint hep-ph/9711456*, 1997.
- [44] S. O. Bilson-Thompson, F. Markopoulou, and L. Smolin, “Quantum gravity and the standard model,” *Classical and Quantum Gravity*, vol. 24, no. 16, p. 3975, 2007.
- [45] B. Kalhor and F. Mehrparvar, “Where is antimatter?” *Available at SSRN 3588471*, 2020.

- [46] M. Dine and A. Kusenko, “Origin of the matter-antimatter asymmetry,” *Reviews of Modern Physics*, vol. 76, no. 1, p. 1, 2003.
- [47] G. Bellini, L. Ludhova, G. Ranucci, and F. Villante, “Neutrino oscillations,” *Advances in High Energy Physics*, vol. 2014, no. 1, p. 191 960, 2014.
- [48] M. Li, X.-D. Li, S. Wang, and Y. Wang, “Dark energy,” *Communications in theoretical physics*, vol. 56, no. 3, p. 525, 2011.
- [49] M. S. Turner, “Dark matter: Theoretical perspectives,” *Proceedings of the National Academy of Sciences*, vol. 90, no. 11, pp. 4827–4834, 1993.
- [50] L. Roszkowski, E. M. Sessolo, and S. Trojanowski, “Wimp dark matter candidates and searches—current status and future prospects,” *Reports on Progress in Physics*, vol. 81, no. 6, p. 066 201, 2018.
- [51] B. Bellazzini, A. Mariotti, D. Redigolo, F. Sala, and J. Serra, “R-axion at colliders,” *Physical review letters*, vol. 119, no. 14, p. 141 804, 2017.
- [52] J. E. Kim and G. Carosi, “Axions and the strong c p problem,” *Reviews of Modern Physics*, vol. 82, no. 1, p. 557, 2010.
- [53] S. Dodelson and L. M. Widrow, “Sterile neutrinos as dark matter,” *Physical Review Letters*, vol. 72, no. 1, p. 17, 1994.
- [54] M. Fabbrichesi, E. Gabrielli, and G. Lanfranchi, *The physics of the dark photon: a primer*. Springer, 2021.
- [55] S. Dawson, “The mssm and why it works,” *Supersymmetry, Supergravity and Supercolliders: TASI*, vol. 97, p. 261, 1997.
- [56] A. Albert, M. Bauer, J. Brooke, *et al.*, “Towards the next generation of simplified dark matter models,” *Physics of the dark universe*, vol. 16, pp. 49–70, 2017.
- [57] S. Abe, G.-C. Cho, and K. Mawatari, “Probing a degenerate-scalar scenario in a pseudoscalar dark-matter model,” *Physical Review D*, vol. 104, no. 3, p. 035 023, 2021.
- [58] M. Backović, M. Krämer, F. Maltoni, A. Martini, K. Mawatari, and M. Pellen, “Higher-order qed predictions for dark matter production at the lhc in simplified models with s-channel mediators,” *The European Physical Journal C*, vol. 75, pp. 1–20, 2015.
- [59] S. Kraml, U. Laa, K. Mawatari, and K. Yamashita, “Simplified dark matter models with a spin-2 mediator at the lhc,” *The European Physical Journal C*, vol. 77, pp. 1–14, 2017.
- [60] European Space Agency, *Planck CMB*, 2013. [Online]. Available: https://www.esa.int/ESA_Multimedia/Images/2013/04/Planck_CMB_black_background.
- [61] XENON Collaboration, *XENON Experiment*, Accessed: 2024. [Online]. Available: <https://xenonexperiment.org/>.
- [62] J. Angle, E. Aprile, F. Arneodo, *et al.*, “Search for light dark matter in xenon10 data,” *Physical Review Letters*, vol. 107, no. 5, p. 051 301, 2011.
- [63] E. Aprile, M. Alfonsi, K. Arisaka, *et al.*, “Dark matter results from 225 live days of xenon100 data,” *Physical review letters*, vol. 109, no. 18, p. 181 301, 2012.

- [64] E. Aprile, J. Aalbers, F. Agostini, *et al.*, “*222*rnemanationmeasurementsforthexenon1texperiment,” *The European Physical Journal C*, vol. 81, no. 4, pp. 1–14, 2021.
- [65] E. Aprile, J. Aalbers, F. Agostini, *et al.*, “Search for coherent elastic scattering of solar b 8 neutrinos in the xenon1t dark matter experiment,” *Physical review letters*, vol. 126, no. 9, p. 091 301, 2021.
- [66] E. Aprile, J. Aalbers, F. Agostini, *et al.*, “Projected wimp sensitivity of the xenonnt dark matter experiment,” *Journal of Cosmology and Astroparticle Physics*, vol. 2020, no. 11, p. 031, 2020.
- [67] Centre for Dark Matter, *WISP Detection*, Accessed: 2024. [Online]. Available: <https://www.centredarkmatter.org/all/wisp-detection-3m3km-2g574-917bh-pz8rz-m7bxg-s5ncg-rdmpe-86kfh-9kp9d-cnmar-tery9-6eghk-yft6m>.
- [68] A. Quiskamp, B. T. McAllister, P. Altin, E. N. Ivanov, M. Goryachev, and M. E. Tobar, “Direct search for dark matter axions excluding alp cogenesis in the 63-to 67- μ ev range with the organ experiment,” *Science advances*, vol. 8, no. 27, eabq3765, 2022.
- [69] B. McAllister, “‘the organ experiment’and other axion dark matter detection techniques,” 2019.
- [70] B. T. McAllister, A. Quiskamp, C. A. O’Hare, *et al.*, “Limits on dark photons, scalars, and axion-electromagnetodynamics with the organ experiment,” *Annalen der Physik*, vol. 536, no. 1, p. 2 200 622, 2024.
- [71] SABRE Collaboration, *SABRE Experiment*, Accessed: 2024. [Online]. Available: <https://www.sabre-experiment.org.au/>.
- [72] University of Sydney, *Sydney Ultra Precision Engineering Laboratory*, Accessed: 2024. [Online]. Available: <https://www.supl.org.au/>.
- [73] University of Hawaii, *Cygnus Experiment*, Accessed: 2024. [Online]. Available: <https://www.phys.hawaii.edu/cygnus/>.
- [74] University of Washington, *Axion Dark Matter eXperiment (ADMX)*, Accessed: 2024. [Online]. Available: <https://depts.washington.edu/admx/>.
- [75] W. Atwood, A. A. Abdo, M. Ackermann, *et al.*, “The large area telescope on the fermi gamma-ray space telescope mission,” *The Astrophysical Journal*, vol. 697, no. 2, p. 1071, 2009.
- [76] C. Meegan, G. Lichti, P. Bhat, *et al.*, “The fermi gamma-ray burst monitor,” *The Astrophysical Journal*, vol. 702, no. 1, p. 791, 2009.
- [77] S. Murgia, “The fermi–lat galactic center excess: Evidence of annihilating dark matter?” *Annual Review of Nuclear and Particle Science*, vol. 70, no. 1, pp. 455–483, 2020.
- [78] M. Di Mauro, M. Stref, and F. Calore, “Investigating the effect of milky way dwarf spheroidal galaxies extension on dark matter searches with fermi-lat data,” *Physical Review D*, vol. 106, no. 12, p. 123 032, 2022.

- [79] T. Jogler and S. Funk, “Revealing w51c as a cosmic ray source using fermi-lat data,” *The Astrophysical Journal*, vol. 816, no. 2, p. 100, 2016.
- [80] M. Ackermann, M. Ajello, A. Albert, *et al.*, “Anisotropies in the diffuse gamma-ray background measured by the fermi lat,” *Physical Review D—Particles, Fields, Gravitation, and Cosmology*, vol. 85, no. 8, p. 083007, 2012.
- [81] B. Penning, “The pursuit of dark matter at colliders—an overview,” *Journal of Physics G: Nuclear and Particle Physics*, vol. 45, no. 6, p. 063001, 2018.
- [82] A. Horvath, *LHC Diagram*, Wikimedia Commons, Accessed: 2024. [Online]. Available: <https://commons.wikimedia.org/wiki/File:LHC.svg>.
- [83] S. Giagu, “Wimp dark matter searches with the atlas detector at the lhc,” *Frontiers in Physics*, vol. 7, p. 75, 2019.
- [84] D. Abercrombie, N. Akchurin, E. Akilli, *et al.*, “Dark matter benchmark models for early lhc run-2 searches: Report of the atlas/cms dark matter forum,” *Physics of the Dark Universe*, vol. 27, p. 100371, 2020.
- [85] J. Alwall, M. Herquet, F. Maltoni, O. Mattelaer, and T. Stelzer, “Madgraph 5: Going beyond,” *Journal of High Energy Physics*, vol. 2011, no. 6, pp. 1–40, 2011.
- [86] R. Ciesielski and K. Goulianos, “Mbr monte carlo simulation in pythia8,” *arXiv preprint arXiv:1205.1446*, 2012.
- [87] C. Arina, J. Heisig, F. Maltoni, *et al.*, “Studying dark matter with maddm 3.1: A short user guide,” *arXiv preprint arXiv:2012.09016*, 2020.
- [88] M. Backović, A. Martini, O. Mattelaer, K. Kong, and G. Mohlabeng, “Direct detection of dark matter with maddm v. 2.0,” *Physics of the Dark Universe*, vol. 9, pp. 37–50, 2015.
- [89] X. Collaboration, E. Aprile, J. Aalbers, *et al.*, “Dark matter search results from a one ton-year exposure of xenon1t,” *Physical review letters*, vol. 121, no. 11, p. 111302, 2018.
- [90] C. Arina, J. Heisig, F. Maltoni, D. Massaro, and O. Mattelaer, “Indirect dark-matter detection with maddm v3. 2–lines and loops,” *The European Physical Journal C*, vol. 83, no. 3, pp. 1–23, 2023.
- [91] J. Heisig, C. Arina, F. Maltoni, *et al.*, “Studying dark matter with maddm 3.1: A short user guide,” *POS PROCEEDINGS OF SCIENCE*, pp. 1–20, 2021.
- [92] T. Sjöstrand, S. Mrenna, and P. Skands, “A brief introduction to pythia 8.1,” *Computer Physics Communications*, vol. 178, no. 11, pp. 852–867, 2008.
- [93] C. Bierlich, A. Buckley, J. Butterworth, *et al.*, “Robust independent validation of experiment and theory: Rivet version 4 release note,” *arXiv preprint arXiv:2404.15984*, 2024.
- [94] A. Buckley, J. Butterworth, D. Grellscheid, *et al.*, “Rivet user manual,” *Computer Physics Communications*, vol. 184, no. 12, pp. 2803–2819, 2013.

Abstract

Abstract : Dark Matter is considered as one of the biggest puzzles in our universe which the SM failed to explain its nature, That's why we used the Simplified Dark Matter models, These models associated with three mediators and new particles have the necessary properties to be Dark Matter candidates, We've simulated the Direct Detection for this models, And the Relic density to get the required mass which make the results compatible with Lambda-CDM Model and astrophysical observations. , After that we simulate the this models in the Large Hadron Collider (LHC) and calculate the (MET)

Keywords : Dark Matter, MOND, Direct Detection, Indirect Detection, Relic Density, LHC, SDMMs, Wimp, MET, Lambda-CDM

Resume : La matière noire est considérée comme l'un des plus grands mystères de notre univers, que le Modèle Standard n'a pas réussi à expliquer. C'est pourquoi nous utilisons les modèles simplifiés de matière noire. Ces modèles sont associés à trois médiateurs et de nouvelles particules ayant les propriétés nécessaires pour être des candidats à la matière noire. Nous avons simulé la détection directe pour ces modèles, ainsi que la densité relique pour obtenir la masse requise qui rend les résultats compatibles avec le modèle Lambda-CDM et les observations astrophysiques. Ensuite, nous simulons ces modèles au Grand Collisionneur de Hadrons (LHC) et calculons le (MET).

Mots-clés : Matière Noire, MOND, Détection Directe, Détection Indirecte, Densité Relique, LHC, Modèles Simplifiés de Matière Noire (SDMMs), WIMP, MET, Lambda-CDM

ملخص : تعتبر المادة المظلمة من أكبر ألغاز كوننا و التي يعجز النموذج المعياري لفيزياء الجسيمات عن تفسير طبيعتها لذلك قمنا في هذا العمل بالإستعانة بثلاث نماذج جديدة تسمى بالنماذج المبسطة للمادة المظلمة, تتضمن بوزونات حاملة للتفاعل و جسيمات تمتلك الخواص اللازمة لتكون مرشحة لحل المشكلة, قمنا بعمل محاكاة للكثافة الكونية المتبقية لهاته الجسيمات المرشحة من أجل إيجاد الكتل التي يجب أن تمتلكها حتى تتوافق النتائج مع النموذج القياسي لعلم الكونيات , بعد ذلك عملنا محاكاة هاته الجسيمات في مصادم الهادرونات الكبير و حسبنا الطاقة الضائعة

الكلمات المفتاحية : المادة المظلمة, النموذج المعياري, الرصد المباشر, الرصد الغير مباشر, الكثافة الكونية المتبقية , نماذج المادة المظلمة المبسطة, جسيمات التفاعل الضعيف, النموذج القياسي لعلم الكونيات, الطاقة الضائعة